Process NMR Associates, LLC
84 Patrick Lane, Ste 115, Poughkeepsie, NY 12603
www.process-nmr.com

TECHNICAL WHITE PAPER · ADDENDUM
PNA-WP-2026-HOPS-01-A1

NMR Spectroscopy in the Analysis of Hops
(*Humulus lupulus* L.)

Addendum Version for Direct qNMR and Chemometrics

Direct qNMR of 49 Hop Samples through a TMS-Transferred Dimethyl Sulfone Calibration, Audit of the Hydroxyl-Region Assignments from the Spectra, and Chemometric Analysis of the Integral and Component Data Sets by Chemistry and Geographic Source

John C. Edwards, Ph.D.
Process NMR Associates, LLC
84 Patrick Lane, Ste 115, Poughkeepsie, NY 12603

Addendum A1.0 · September 23, 2026
To be incorporated into PNA-WP-2026-HOPS-01 (version 1.1, September 20, 2026)

Document Details

Document number	PNA-WP-2026-HOPS-01-A1 (addendum to PNA-WP-2026-HOPS-01; number assigned on the pattern of the PNA white paper series, to be confirmed by the author)
Title	NMR Spectroscopy in the Analysis of Hops (Humulus lupulus L.). Addendum A1: Direct Quantitative ^{1}H NMR and Chemometrics: Direct qNMR of 49 Hop Samples through a TMS-Transferred Dimethyl Sulfone Calibration, Audit of the Hydroxyl-Region Assignments from the Spectra, and Chemometric Analysis of the Integral and Component Data Sets by Chemistry and Geographic Source
Version and date	Addendum Version for Direct qNMR and Chemometrics (A1.0), September 23, 2026. Written to be incorporated into the main paper in a later version (see Section A10 for the proposed placement).
Parent document	PNA-WP-2026-HOPS-01 (version 1.1, September 20, 2026)
Author and organization	John C. Edwards, Ph.D., Process NMR Associates, LLC, 84 Patrick Lane, Ste 115, Poughkeepsie, NY 12603 (www.process-nmr.com)
File name	PNA-WP-2026-HOPS-01-A1_Direct_qNMR_and_Chemometrics.docx
Companion files	PNA-WP-2026-HOPS-01-A1_Companion_Workbook.xlsx (all inputs, the qNMR calculation with live formulas, the four chemometric data matrices, pretreatment comparison, scores, loadings, clusters, embeddings, classification and permutation results, and the verified reference list); PNA-WP-2026-HOPS-01-A1_3D_Score_Viewer.html (interactive three-dimensional PCA, UMAP and t-SNE score plots; runs in any web browser without installation).
AI assistance	This document was drafted with the assistance of Claude (Anthropic) working in a Cowork session. Model identifier as reported by the session: claude-opus-5-5; the model actually serving individual turns may differ from the configured identifier. Reasoning-effort setting: not declared by the author and therefore not recorded.
Tools engaged	pdfplumber (text-layer, vector-path and integral-region-bar extraction from the supplied spectra); NumPy 2.4, SciPy 1.17 and pandas 3.0 (digitization, pseudo-Voigt line fitting, qNMR calculation, bootstrap and uncertainty analysis); scikit-learn 1.8 and umap-learn 0.5 (PCA, clustering, t-SNE, UMAP, classifiers, nested cross-validation and permutation tests); matplotlib 3.10 (figures); Plotly 7.1 (interactive viewer); openpyxl and LibreOffice (workbook build and formula recalculation); CrossRef REST API, Europe PMC and publisher and standards-body web pages (reference verification); Node.js docx 9.6.1 (document build); LibreOffice and Poppler (render check). Python 3.11; all random seeds fixed.
Division of content	AI-performed: extraction and digitization of the supplied spectra, recovery of the exact integration windows, line fitting, the qNMR calculations and bottle-assignment tests, the uncertainty budget, the statistical assignment of the minor windows, all chemometric and machine-learning analyses with their interpretation, the figures, tables, interactive viewer, companion workbook and the narrative text. Author-supplied: all NMR spectra with their integral tables, sample masses, the DMS masses and bottle assignments, sample labels and declared α-acid contents, the ICE-4 spectrum, and the DMS purity (PNA terpene-assay worksheet). Conclusions drawn from the PNA data are offered for the author's review and adoption.
Revision history	A1.0 (September 23, 2026): first issue of the addendum.
Reference verification	59 references are cited: 50 journal articles whose authors, title, journal, year, volume, pages and DOI were verified against the CrossRef registry; 2 book chapters verified against CrossRef; 5 items (two open-access journal articles without DOIs, a BIPM report and two supplier product pages) verified at their source; and 2 ASBC methods of analysis cited from version 1.1. 8 of the journal articles were read in full from the project library and the abstracts of 6 others were examined; the remainder, chiefly methodological references, are cited only for methods or statements evident from their verified bibliographic records.

Abstract

The 300 MHz ^{1}H NMR spectra of $CDCl_3$ extracts of 49 hop samples, comprising the 36 retail samples of the survey examined in version 1.1 of PNA-WP-2026-HOPS-01 and 13 further samples (five Cryo pellets, six New Zealand hops and two harvests of HBC 1019), were integrated over one fixed set of 22 windows and normalized to the tetramethylsilane (TMS) signal of the extraction solvent. Because no calibrant had been added to the sample tubes, the absolute scale was established by a transfer calibration: dimethyl sulfone (DMS) was weighed into 800 µL of each of the two bottles of $CDCl_3$ used for the extractions, and the TMS signal of each sample spectrum was made to carry the DMS calibration of its bottle. The two bottles were found to differ by a factor of 2.20 in TMS content (1.29 and 2.85 mM), so that the TMS content of an opened bottle cannot be taken as known. The assignment of samples 038–050 to the bottle containing 8.74 mg of DMS was confirmed by the agreement of their α-acid contents with the declared values (mean ratio 1.04, range 0.82–1.23, against 0.47 under the alternative), and those samples were retained in the quantitative analysis. α-Acid contents of 0.82–25.96 % and β-acid contents of 1.09–13.48 % (w/w, as is) were obtained, and the older retail samples were found to contain about three quarters of their declared α-acids, as storage losses would lead one to expect. The ICE-4 calibration extract reproduced its certified homolog composition to within one percentage point and its α/β ratio to within 6.5 %, but its absolute contents failed the check, most probably through an error in the recorded mass or bottle; the absolute contents are therefore regarded as provisional to within about ±10 %, against a root-sum-square of the quantified uncertainty components of 2.9–3.8 %.

The resolved spectra confirmed the assignments that version 1.1 had inferred from its integral list. The minor tautomers of the three β-acids stand in the same ratio, about 0.45, to their major forms, the pair of signals at δ 18.537 and 18.511 is tied in fixed proportion to colupulone and lupulone respectively, and the ICE-4 spectrum settled the counting rule for the β-acids in favor of the major plus minor tautomers. The α-acid hydroxyl signals were shown to move to low field with increasing concentration, which, according to line fitting, biases the fixed-window adhumulone fraction of the concentrated Cryo extracts high by 3.7–5.0 percentage points and their cohumulone fraction low by 1.0–4.8 points.

The chemometric analysis was applied to the integrals and to the quantified constituents, each on the absolute scale and as composition, after a comparison of sixty pretreatments in which mean-centering with Pareto scaling proved the most robust, and in which level scaling and the generalized logarithm allowed a blank window to generate a spurious separation of the two measurement campaigns. Principal component analysis, Ward clustering, UMAP and *t*-SNE organized the samples by amount, α/β ratio, co-homolog fraction and oil content, and three chemotypes, β-rich, high-cohumulone and α-rich, were resolved that follow the lineage of the cultivars rather than the country of growth; the nonlinear maps preserved local neighborhoods less faithfully than three principal components. Under leave-one-cultivar-out validation with permutation testing, the best of eight classifiers, which included PLS-DA and support vector machines, recognized the product form almost perfectly from the absolute data (balanced accuracy 0.99), whereas the region of growth and the region of breeding were recognized only weakly (0.34–0.61, chance 0.33) and, although the best models exceeded their permutation distributions, no better, to within a few hundredths, than by a baseline model given only three chemical descriptors. The ^{1}H NMR data measure the genotype and the history of the product, not its geographic origin. Recommendations are made for securing the absolute scale, for validating the method and for designing a study capable of testing geographic origin. Fifty-nine references are cited, each verified against its registry record or its source.

Table of Contents

A1. Introduction and Scope 6
A2. Samples, Spectra and Data Handling 7
A2.1 The Two Sample Sets 7
A2.2 Geographic and Genetic Metadata 7
A2.3 Extraction of the Data from the Spectra 9
A2.4 Observations on Data Integrity 9
A3. The Integration Windows and the Assignment of the Hydroxyl Region 9
A3.1 Windows and Observed Signal Positions 9
A3.2 The Concentration Dependence of the α-Acid Hydroxyl Shifts 12
A3.3 Line Shapes and the Capture of Each Signal by Its Window 13
A3.4 Statistical Assignment of the Minor Windows with 49 Samples 13
A3.5 The ICE-4 Test Proposed in Version 1.1 15
A3.6 The Terpene Windows 16
A4. Direct qNMR through a TMS-Transferred Dimethyl Sulfone Calibration 16
A4.1 Principle 16
A4.2 The Calibration of the Two Bottles 17
A4.3 Assignment of the Samples to the Bottles and the Test of the 8.74 mg Assumption 18
A4.4 Results 20
A4.5 The ICE-4 Extract as an Absolute Check 22
A4.6 Same-Cultivar Comparisons 23
A4.7 The Co-Homolog Relationship 24
A4.8 Terpenes 24
A5. Uncertainty of the Calibration Route and Audit of the Method 25
A6. Design of the Chemometric Analysis 27
A6.1 Two Views of One Measurement 27
A6.2 Pretreatments 27
A6.3 Methods 28
A7. Choice of Pretreatment 29
A8. Unsupervised Analysis 31
A8.1 Principal Components of the Integral Data 31
A8.2 Principal Components of the Component Data 33
A8.3 Hierarchical Clustering: Chemotypes and Content Classes 34
A8.4 UMAP and t-SNE 37
A8.5 Geography in the Unsupervised Maps 40
A9. Supervised Classification 40
A9.1 The Positive Control: Product Form 40
A9.2 Region of Growth and Region of Breeding 40
A9.3 Confounding 42
A9.4 What the Classifiers Use 43
A9.5 The Trade Classification 44
A9.6 Interpretation 44
A10. What the Addendum Changes in Version 1.1 45

A11. Critical Assessment and Recommendations 46
A11.1 What a Reviewer or an Opposing Expert Would Raise 46
A11.2 Recommendations 47
A12. Conclusions 48
References 49
Summary 52

A1. Introduction and Scope

The first issue of this white paper, PNA-WP-2026-HOPS-01, and its revision 1.1 examined the hydroxyl region of the 300 MHz ^{1}H spectra of $CDCl_3$ extracts of 36 commercial hop samples, together with a five-sample combined HPLC–NMR study, and applied chemometric and machine-learning methods to the integrals. Three limitations of that material were stated repeatedly and governed every conclusion drawn from it. The integrals had been archived after division by the adlupulone signal, so that the absolute scale of the spectra had been lost and only the composition of the bitter-acid fraction could be analyzed; the integration windows were not available, so that the identity of each integral had to be inferred from its position in a list and from its statistical behavior; and no internal calibrant had been present, so that contents could not be obtained from the NMR data at all. It was concluded that no model built on relative integrals could stand in place of an internal standard, and the re-integration of the survey with one documented window set and with the integrals archived on an absolute scale was listed among the tasks reserved for a later version.

That task has now been carried out, and the data set has been enlarged. The spectra themselves have been supplied, each with a table of twenty-two integrals over one fixed set of windows: eighteen windows spanning the chelated enolic hydroxyl region between δ 19.36 and 18.02, three windows in the olefinic region carrying the diene signal of myrcene and the H-3 signal of α-humulene, and the tetramethylsilane (TMS) signal, which was set to ten integration units in every spectrum. Thirteen further samples were added: five Cryo (lupulin-enriched) pellets of US cultivars, six New Zealand hops including three harvests of Wakatu, and two harvests of the experimental cultivar HBC 1019. Because no calibrant was added to the sample tubes, the absolute scale was established indirectly. Dimethyl sulfone (DMS) was weighed into 800 µL of each of the two bottles of TMS-containing $CDCl_3$ that had been used for the extractions, the DMS integral was recorded with the TMS signal set to ten, and the same 800 µL volume was used for every extraction, so that the TMS signal of each sample spectrum could serve as a transfer standard carrying the DMS calibration of its bottle. The spectrum of the ASBC ICE-4 calibration extract was recorded in the same campaign.

The addendum has five objectives. The first is to carry out the quantitative NMR calculation for all 49 samples on the basis of the TMS-transferred DMS calibration, and to test, against the α-acid contents declared on the packages, the assumption that samples 038–050 were extracted with the second bottle (8.74 mg of DMS in 800 µL), with the instruction that those samples be withdrawn from the quantitative analysis if the comparison should show the assumption to be wrong. The second is to audit the integration windows and the assignments of v1.1 against the spectra, which were not available when those assignments were made. The third is to establish the uncertainty of the new calibration route and the ways in which it can fail. The fourth is to apply chemometric methods, principal component analysis (PCA), hierarchical cluster analysis (HCA), uniform manifold approximation and projection (UMAP), *t*-distributed stochastic neighbor embedding (*t*-SNE), support vector machines (SVM), partial least-squares discriminant analysis (PLS-DA) and several other classifiers, to two views of the same measurements, the integrals as recorded and the quantified chemical components, with an explicit comparison of pretreatments and with groupings examined by chemistry and by geographic source. The fifth is to state what the new data confirm, revise or overturn in v1.1, so that the addendum can later be incorporated into the main paper.

The addendum is written to stand alone, but it does not repeat the background of the main paper on hop chemistry, the published assignments of the bitter acids or the literature on quantitative NMR of hops,[1–4] which should be consulted for those subjects. Sections, tables and figures are numbered with the prefix A so that they can be inserted into the main paper without renumbering. All input data, calculations and

outputs are provided in the companion workbook, and the three-dimensional score plots are provided as an interactive file that runs in any web browser.

A2. Samples, Spectra and Data Handling

A2.1 The Two Sample Sets

The samples fall into two sets that differ in age, in provenance and in the way the spectra were recorded, and the distinction has to be kept in view throughout. Set S1 comprises the 36 retail samples, numbered 001–036, of 33 cultivars that formed the survey of v1.1; Belma, Hersbrucker and Magnum each occur twice. Set S2 comprises 13 samples numbered 038–050: Cryo pellets of Centennial, Amarillo, Cascade, Simcoe and Mosaic from Yakima Chief Hops, which are produced by cryogenic separation of the lupulin glands from the bract and are stated by the supplier to carry roughly twice the lupulin load of type-90 pellets;[5] New Zealand Wakatu of the 2022, 2023 and 2024 harvests, Nelson Sauvin and Waimea of 2023 and Nectaron of 2024; and the experimental Yakima cultivar HBC 1019 of the 2022 and 2024 harvests. Five cultivars occur in both sets: Cascade, Centennial and Amarillo, each as a retail pellet in S1 and a Cryo pellet in S2, and Nelson Sauvin and Waimea, as retail pellets in both. In all, 49 samples of 38 cultivars were examined, ten cultivars being represented by two or three samples.

Approximately 100 mg of each sample (95.00–112.67 mg, recorded to 0.1 mg in S1 and to 0.01 mg in S2) was extracted into 800 µL of $CDCl_3$ containing TMS, and the ^1H spectrum was recorded on the Varian Mercury-MVX 300 spectrometer with a relaxation delay of 15 s; the spectra of S2 carry the additional annotation of a 15 kHz spectral width. The pulse angle, acquisition time, number of transients, probe temperature, extraction time and filtration step are not recorded in the material supplied, and the harvest year is known only for eight samples of S2. The acquisition dates are not recorded either. The S1 series is the one archived for v1.1, and its lower bitter-acid and oil contents relative to the declared values (Section A4) suggest that its samples are older or were stored less well, but that is an inference and not a recorded fact.

A2.2 Geographic and Genetic Metadata

The country of growth was printed on 28 of the 49 labels. For the remaining 21 it was inferred from the cultivar or the supplier, and for three samples, the Hallertau (024), the second Magnum (026) and the Perle (029), the inference is weak, since each of these cultivars is grown commercially both in Germany and in the United States. Two geographic descriptors were therefore defined and used side by side: the region of growth (Europe, 15 samples; North America, 24; Oceania, 10), which rests partly on inference, and the region in which the cultivar was bred (Europe, 16; USA, 23; Oceania, 10), which is a property of the cultivar and is known for every sample. The two differ for Northern Brewer, an English cultivar grown here in the United States. The sample metadata are given in Table A1, in which the basis of every country assignment is stated.

Table A1. The 49 hop samples: cultivar (harvest year where printed), declared α-acid content, country of growth with the basis of its assignment, region of growth, region in which the cultivar was bred, product form, measurement set and solvent bottle, and mass extracted.

ID	Cultivar	Declared α (%)	Country (basis)	Region of growth	Bred in	Form	Set / bottle	Mass (mg)
001	Magnum	12.3	Germany (L)	Europe	Europe	pellet	S1 / B	102.40
002	Galena	11.6	USA (L)	North America	USA	pellet	S1 / B	96.10
003	Vic Secret	16.5	Australia (L)	Oceania	Oceania	pellet	S1 / A	97.40

ID	Cultivar	Declared α (%)	Country (basis)	Region of growth	Bred in	Form	Set / bottle	Mass (mg)
004	Idaho 7	13.4	USA (L)	North America	USA	pellet	S1 / A	101.50
005	Ariana	10.4	Germany (L)	Europe	Europe	pellet	S1 / B	102.80
006	Sterling	6.5	USA (L)	North America	USA	pellet	S1 / B	100.10
007	Summit	14.0	USA (L)	North America	USA	pellet	S1 / A	100.80
008	Nelson Sauvin	10.5	New Zealand (L)	Oceania	Oceania	pellet	S1 / B	106.60
009	German (unspecified)	3.5	Germany (L)	Europe	Europe	pellet	S1 / B	99.80
010	Waimea	14.5	New Zealand (L)	Oceania	Oceania	pellet	S1 / A	101.80
011	Azacca	13.6	USA (L)	North America	USA	pellet	S1 / B	104.50
012	Crystal	2.2	USA (L)	North America	USA	pellet	S1 / B	100.90
013	Traditional German	5.1	Germany (N)	Europe	Europe	pellet	S1 / A	98.50
014	Enigma	16.7	Australia (L)	Oceania	Oceania	pellet	S1 / B	108.30
015	Sultana	12.4	USA (C)	North America	USA	pellet	S1 / A	104.00
016	Bravo	14.2	USA (L)	North America	USA	pellet	S1 / A	102.80
017	Northern Brewer	5.8	USA (L)	North America	Europe	pellet	S1 / A	104.90
018	Centennial	10.1	USA (C)	North America	USA	pellet	S1 / A	96.20
019	Saaz	2.8	Czechia (L)	Europe	Europe	pellet	S1 / A	97.60
020	Chinook	13.2	USA (C)	North America	USA	pellet	S1 / A	95.00
021	Spalt	2.1	Germany (L)	Europe	Europe	pellet	S1 / B	111.10
022	Amarillo	9.2	USA (L)	North America	USA	pellet	S1 / A	102.00
023	Savinjski Golding	2.6	Slovenia (C)	Europe	Europe	pellet	S1 / A	107.60
024	Hallertau	2.8	Germany (C?)	Europe	Europe	pellet	S1 / A	105.50
025	Belma	8.9	USA (C)	North America	USA	pellet	S1 / A	111.20
026	Magnum	8.9	Germany (C?)	Europe	Europe	pellet	S1 / A	95.40
027	Cluster	7.4	USA (L)	North America	USA	pellet	S1 / B	104.50
028	Hersbrucker	1.7	Germany (C)	Europe	Europe	pellet	S1 / A	106.50
029	Perle	5.1	Germany (C?)	Europe	Europe	pellet	S1 / A	107.90
030	Hallertau Blanc	7.6	Germany (C)	Europe	Europe	pellet	S1 / A	101.80
031	Herkules	16.6	Germany (C)	Europe	Europe	pellet	S1 / A	96.70
032	Cascade	5.6	USA (C)	North America	USA	pellet	S1 / A	103.40
033	Belma	8.9	USA (C)	North America	USA	pellet	S1 / B	111.20
034	Hersbrucker	1.7	Germany (L)	Europe	Europe	pellet	S1 / B	109.30
035	Nugget	15.3	USA (L)	North America	USA	pellet	S1 / B	96.60
036	Huell Melon	4.3	Germany (L)	Europe	Europe	pellet	S1 / B	101.80
038	Centennial	18.5	USA (S)	North America	USA	Cryo	S2 / B	105.80
039	Amarillo	16.1	USA (S)	North America	USA	Cryo	S2 / B	108.80
040	Cascade	11.9	USA (S)	North America	USA	Cryo	S2 / B	105.90
041	Simcoe	25.6	USA (S)	North America	USA	Cryo	S2 / B	100.30
042	Mosaic	21.6	USA (S)	North America	USA	Cryo	S2 / B	108.34
043	Wakatu (2023)	6.9	New Zealand (L)	Oceania	Oceania	pellet	S2 / B	101.08
044	Nelson Sauvin (2023)	11.4	New Zealand (L)	Oceania	Oceania	pellet	S2 / B	104.48
045	Wakatu (2024)	7.7	New Zealand (L)	Oceania	Oceania	pellet	S2 / B	109.89
046	HBC 1019 (2022)	9.6	USA (C)	North America	USA	pellet	S2 / B	110.52
047	Waimea (2023)	14.3	New Zealand (L)	Oceania	Oceania	pellet	S2 / B	101.17
048	Nectaron (2024)	13.7	New Zealand (L)	Oceania	Oceania	pellet	S2 / B	110.85
049	Wakatu (2022)	5.3	New Zealand (L)	Oceania	Oceania	pellet	S2 / B	112.67
050	HBC 1019 (2024)	11.3	USA (C)	North America	USA	pellet	S2 / B	107.60

Basis: L, printed on the label; N, inferred from the product name; C, inferred from the cultivar; C?, inferred from the cultivar but the cultivar is grown commercially in both Germany and the USA; S, inferred from the supplier. Set S1: samples 001–036 (survey of v1.1);

S2: samples 038–050. Bottle A: 4.5 mg DMS calibration; bottle B: 8.74 mg DMS calibration (Section A4.2). Sample 022 is listed in the bottle workbook as a second 032 (Section A2.4).

A2.3 Extraction of the Data from the Spectra

The integral tables were read from the text layer of the vector PDF files in which the spectra were supplied and were cross-checked against the printed values. The absolute integrals were used throughout, and every table was re-normalized so that the TMS window (δ 0.12 to −0.12) equals ten units. This step was necessary because the normalized column printed on four of the spectra, those of samples 025, 038 and 040 and of ICE-4, refers to a different reference value; in the other 46 spectra the TMS signal had been printed equal to ten. The integration limits printed in the tables are rounded to 0.01 ppm, and the exact limits were recovered from the integral region bars drawn beneath each spectrum. They are identical in all 50 spectra to within 0.0001 ppm and are listed in Table A2; the boundary between the adhumulone and cohumulone windows, for example, lies at δ 19.0140 and not at 19.01 as printed.

The spectrum traces are themselves stored as vector paths of 475–2,014 points over 1.85–2.15 ppm, and they were digitized with the chemical-shift axis calibrated on the printed scale. Integration of the digitized traces over the recovered limits reproduced the printed integrals with a standard deviation of 0.05–0.17 % of the summed major signals in every window except the broad window W10 (0.42 %), which validates the traces for the measurement of peak positions and for line fitting (Section A3). Peaks that run off the top of the printed plot, as the humulone signal does in many spectra, were excluded from any quantity that depends on their height. Four representative spectra are reproduced from the digitized traces in Figure A1.

A2.4 Observations on Data Integrity

Several irregularities were found while the data were assembled, and each has a bearing on what follows. The workbook that assigns the samples to the two bottles of $CDCl_3$ lists sample 032 twice in the 4.5 mg block and omits sample 022; the second entry has been taken to be 022, an assumption tested and confirmed in Section A4.3. The ICE-4 spectrum is not assigned to either bottle, and its printed mass, 95.4 mg, is identical to that of sample 026. The two Belma samples, 025 and 033, bear the same label and the same recorded mass, 111.2 mg, yet their compositions differ (Section A4.6), so that they cannot be two spectra of one preparation and at least one of the two masses may have been copied. Sample 026, labeled "Magnum 8.9 %", was questioned in v1.1 because its declared value is that of the Belma label beside it, and its composition is examined again below. Two humulene integrals, those of Northern Brewer (017) and Saaz (019), are slightly negative, and the blank window W18, which contains no signal, carries a small positive offset in S2 (0.025 units on the TMS scale, against −0.003 in S1) that is traced to baseline treatment; the consequence of that offset for the chemometric analysis is shown in Section A7.

A3. The Integration Windows and the Assignment of the Hydroxyl Region

A3.1 Windows and Observed Signal Positions

The eighteen hydroxyl-region windows, their exact limits, the positions of the signals observed within them and the assignments adopted in this addendum are collected in Table A2, and the windows are drawn over four spectra in Figure A1. The six major signals fall where the survey assignment of v1.1 had placed them. The major tautomers of the β-acids resonate at δ 19.342 (adlupulone, W1), 19.289 (colupulone, W2) and 19.214 (lupulone, W3), each within ±0.006 ppm in all 50 spectra, and the enolic 3-OH signals of the α-acids at δ 19.029 (adhumulone, W7), 18.998 (cohumulone, W8) and 18.867 (humulone, W9), in agreement with the values reported for lupulin extracts by Killeen and co-workers, 19.35, 19.30, 19.22, 19.03, 19.00

and 18.87.[2] The upfield group contains the three minor tautomers of the β-acids at δ 18.403 (W13), 18.381 (W14) and 18.294 (W16), the latter two as sharp, well-resolved singlets and the first as a smaller line on the low-field flank of the second, in the positions given by Killeen and co-workers for adlupulone, lupulone and colupulone respectively (18.41, 18.39 and 18.30).[2] Between the two groups lies a pair of well-defined singlets at δ 18.537 (W11) and 18.511 (W12), preceded by a cluster of weak lines between δ 18.56 and 18.63 (W10). Weak singlets are also seen at δ 19.181, 19.153 and 19.120 (W4–W6), at δ 18.348 (W15) and at δ 18.231 (W17), and the window W18 (δ 18.07–18.02) contains no signal in any spectrum and serves as a blank.

Table A2. The 22 integration windows: exact limits (W1–W18 recovered from the integral region bars; W19–W22 as printed), median position of the highest point of the digitized trace in each window with its range over 50 spectra (line-fit positions of the α-acid signals are given in Section A3.2), assignment, and non-negative least-squares coefficients of each minor window on the six major signals (per 100 units of the six; bootstrap 95 % interval) with R^2.

Window	Limits δ (ppm)	Peak δ, median (range)	Assignment	NNLS on the six major signals	R^2
W1	19.3581–19.3243	19.342 (19.339–19.344)	Adlupulone, major tautomer	major signal	
W2	19.3243–19.2550	19.289 (19.285–19.292)	Colupulone, major tautomer	major signal	
W3	19.2550–19.1863	19.214 (19.209–19.220)	Lupulone, major tautomer	major signal	
W4	19.1863–19.1671	19.181 (19.172–19.190)	Unassigned chelated enol	none ≥ 0.02	0.22
W5	19.1671–19.1343	19.153 (19.148–19.156)	Unassigned chelated enol	ad-β 0.05 [0.00–0.09]	0.42
W6	19.1343–19.0937	19.120 (19.091–19.123)	Unassigned chelated enol	ad-β 0.07 [0.00–0.13]; co-α 0.02 [0.00–0.03]	0.10
W7	19.0624–19.0140	19.029 (19.011–19.035)	Adhumulone 3-OH	major signal	
W8	19.0140–18.9396	18.998 (18.982–19.010)	Cohumulone 3-OH	major signal	
W9	18.9396–18.8193	18.867 (18.843–18.885)	Humulone 3-OH	major signal	
W10	18.7438–18.5642	18.56–18.63	Cluster of weak lines (α-acid derivatives?)	ad-β 0.16 [0.00–0.86]; co-β 0.16 [0.00–0.30]	0.45
W11	18.5642–18.5226	18.537 (18.535–18.540)	Colupulone-associated (δ 18.5 pair)	co-β 0.24 [0.20–0.27]; n-β 0.05 [0.00–0.09]	0.94
W12	18.5226–18.4784	18.511 (18.510–18.513)	Lupulone-associated (δ 18.5 pair)	n-β 0.21 [0.17–0.23]; co-β 0.03 [0.00–0.05]	0.95
W13	18.4227–18.3951	18.403 (18.402–18.406)	Adlupulone, minor tautomer	ad-β 0.44 [0.34–0.52]; n-β 0.04 [0.01–0.06]	0.97
W14	18.3951–18.3591	18.381 (18.378–18.382)	Lupulone, minor tautomer	n-β 0.41 [0.36–0.44]; ad-β 0.05 [0.00–0.25]	0.99
W15	18.3591–18.3253	18.348 (18.341–18.352)	Colupulone-associated, weak	co-β 0.09 [0.06–0.10]	0.76
W16	18.3253–18.2602	18.294 (18.293–18.299)	Colupulone, minor tautomer	co-β 0.46 [0.41–0.48]; n-β 0.06 [0.01–0.10]	0.96
W17	18.2602–18.1884	18.231 (18.226–18.248)	Unassigned	co-β 0.04 [0.00–0.05]	0.07
W18	18.0702–18.0171	—	Blank (no signal)	none ≥ 0.02	0.06
W19	6.43–6.32	6.37	Myrcene-type diene H-2 (myrcene + β-farnesene + (E)-β-ocimene)	—	
W20	5.66–5.60	5.6	α-Humulene H-3, low-field half	—	
W21	5.60–5.53	5.6	α-Humulene H-3, high-field half (+ other)	—	
W22	0.12 to −0.12	0.00	TMS (set to 10)	—	

ad-β, co-β, n-β: major signals of adlupulone, colupulone and lupulone (W1–W3); ad-α, co-α, n-α: adhumulone, cohumulone and humulone (W7–W9). The S2 spectra used 6.44–6.32, 5.66–5.59 and 5.59–5.52 ppm for W19–W21. $CDCl_3$, 300 MHz; TMS at δ 0.

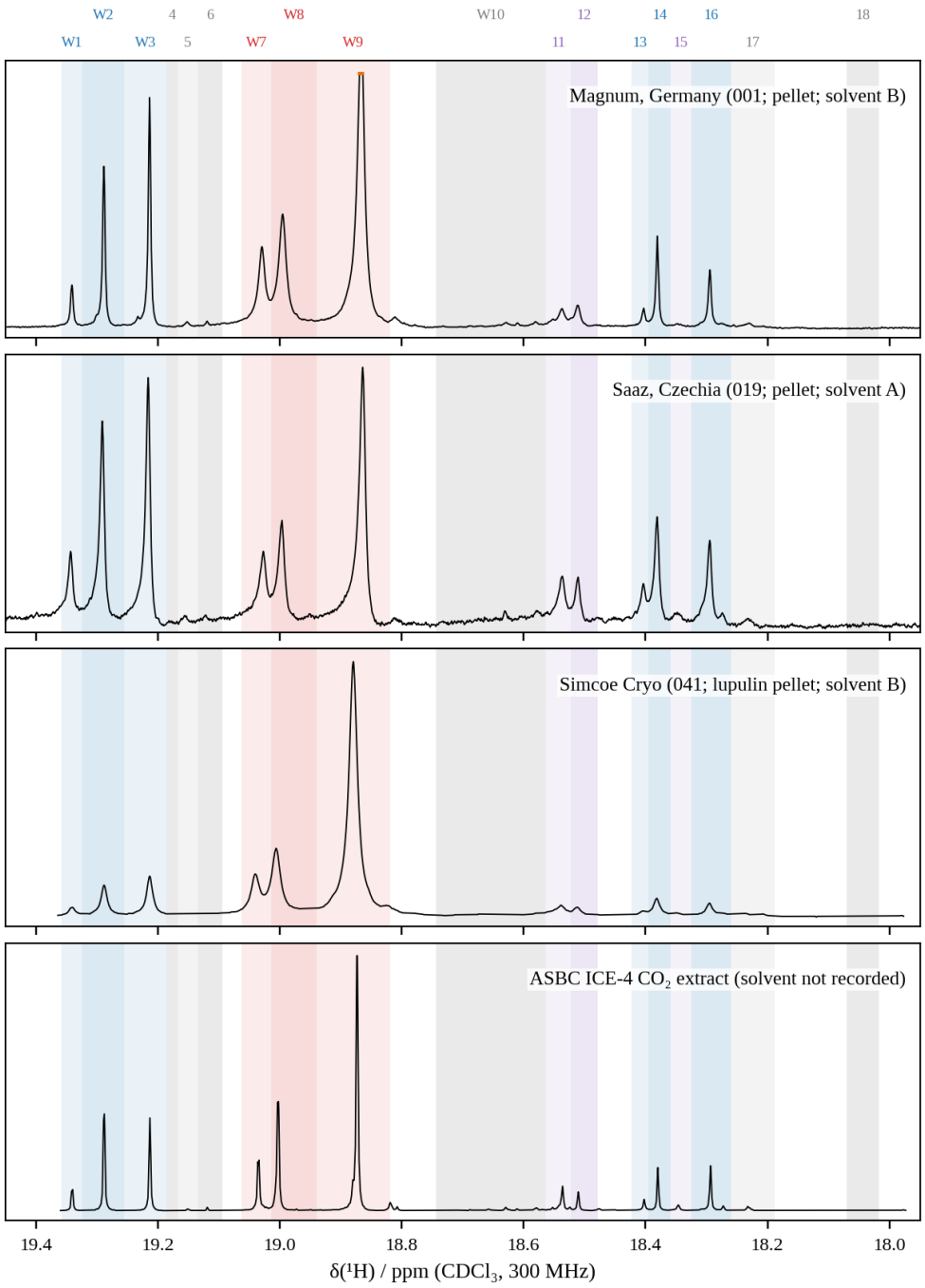

Figure A1. The hydroxyl region of four spectra reproduced from the digitized traces of the supplied PDF files, with the eighteen integration windows at their exact limits (blue: β-acid major and minor tautomers; red: α-acids; violet: the β-associated signals W11, W12 and W15; gray: other windows, including the blank W18). Orange segments mark peaks that ran off the top of the original plot. $CDCl_3$, 300 MHz.

The line widths differ systematically between the two classes of bitter acid, and the difference matters for integration. Pseudo-Voigt fitting of the digitized traces (Section A3.3) gave median full widths at half height of 1.7–1.8 Hz for the major β-acid signals, 1.8–2.2 Hz for the minor tautomers and 3.3–3.4 Hz for the three α-acid signals, with interquartile ranges of 2.7–4.3 Hz for the latter. The α-acid 3-OH signals are therefore broadened by some 1.6 Hz relative to their β-acid counterparts in the hop extracts, whereas in the anhydrous

ICE-4 extract all the hydroxyl lines are sharp (Figure A1). The broadening is most simply attributed to chemical exchange of the α-acid enolic proton with water extracted from the hop, and it was slightly greater in the extracts made with the older, wetter bottle of $CDCl_3$ (median 3.6 Hz against 3.3 Hz for humulone); the lines were close to Lorentzian in shape (median fitted Lorentzian fraction 0.90 for the β-acid lines and 1.00 for the α-acid lines).

A3.2 The Concentration Dependence of the α-Acid Hydroxyl Shifts

The positions of the α-acid signals are not fixed. They move to low field as the concentration of bitter acids in the tube increases (Figure A2a), by 0.018 ppm per 100 mM for humulone (r = 0.82), 0.011 ppm for cohumulone (r = 0.74) and 0.014 ppm for adhumulone (r = 0.86), over a concentration range of 7–118 mM of total bitter acids, whereas the major β-acid signals move slightly to high field (0.003–0.004 ppm per 100 mM) and the minor tautomers, together with W11 and W12, are fixed to within 0.002 ppm. Humulone was thus found by line fitting between δ 18.846 and 18.885, cohumulone between 18.985 and 19.010 and adhumulone between 19.023 and 19.044. The most concentrated extracts are those of the Cryo pellets, in which α-acids alone reach 41–96 mM.

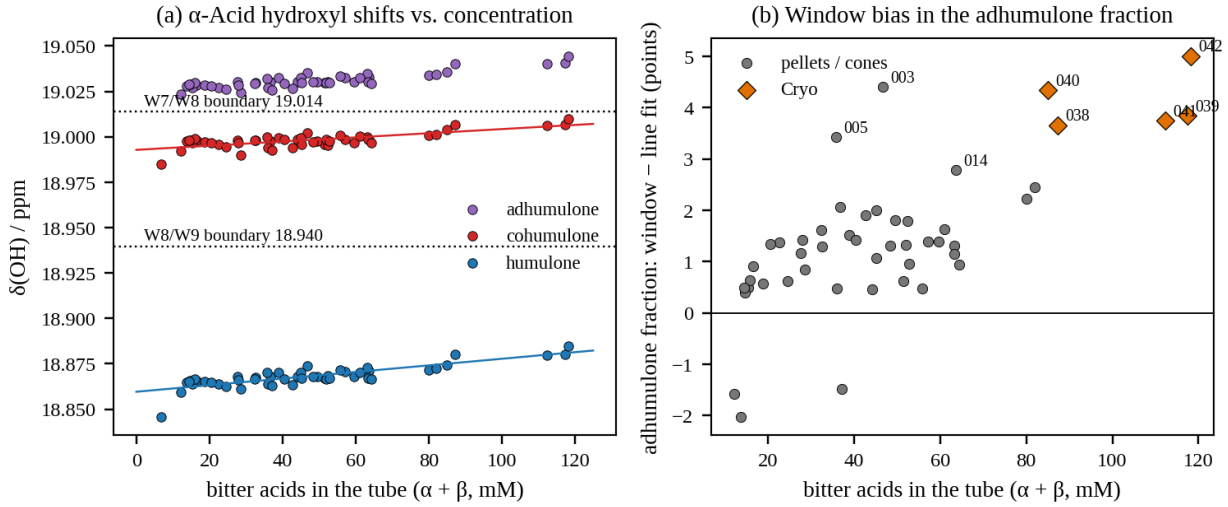

Figure A2. (a) Hydroxyl chemical shifts of the α-acids from line fitting of the digitized spectra against the total concentration of bitter acids in the NMR tube, with the fixed window boundaries at δ 19.014 (W7/W8) and 18.940 (W8/W9). (b) Difference between the adhumulone fraction of the α-acids obtained from the fixed windows and that obtained by line fitting, in percentage points; diamonds denote Cryo pellets.

The consequence for the fixed windows follows directly. The boundary between the adhumulone and cohumulone windows, at δ 19.0140, lies about 5 Hz (4.1–6.0 Hz) to low field of the cohumulone signal in a typical pellet extract but only 1–3 Hz from it in the Cryo extracts, where it cuts into the low-field flank of a line whose half-width at half height is 1.7 Hz. Line fitting of the α-acid triplet shows that the fixed windows overstate the adhumulone fraction of the α-acids by a median of 1.3 percentage points in the pellet extracts and by 3.7–5.0 points in the five Cryo extracts (Figure A2b), and that they understate the cohumulone fraction, by a median of 0.7 points in the pellet extracts and by 1.0–4.8 points in the Cryo extracts, the remainder of the difference falling on humulone. The largest discrepancies in the cohumulone fraction, 4.4–7.4 points, are found in the three pellets with the highest cohumulone content (Vic Secret, Ariana, Enigma), whose adhumulone fraction is also overstated by 2.8–4.4 points, because the wings of the dominant, exchange-broadened cohumulone line then contribute appreciably to both neighboring windows. The α-acid totals are not affected by the placement of the inner boundaries. The cohumulone fractions of

the Cryo pellets and of the high-cohumulone cultivars reported in Section A4 are therefore low by several points, and a direct comparison of a Cryo pellet with a conventional pellet of the same cultivar is biased in the same direction; for Cascade, the line fit places the Cryo pellet at 32.0 % cohumulone against 28.6 % from the windows, which reconciles it with the retail Cascade (31.5 % by the windows, 32.1 % by the fit). The line-fit fractions rest on the assumption that the wings of each line are Lorentzian, and they are not a substitute for a chromatographic reference; they show, however, that the fixed windows are adequate only for extracts of moderate concentration and moderate cohumulone content. Windows set from each spectrum, line fitting of the α-acid triplet, or dilution of the concentrated extracts to the concentration range of the pellets would reduce the problem.

A3.3 Line Shapes and the Capture of Each Signal by Its Window

Because the lines are close to Lorentzian, a significant fraction of the intensity of each signal lies outside a window of the widths used here, which are 8–36 Hz for the windows of the bitter-acid signals. The fraction of each fitted line that falls within its own window was found to be 0.95 for the major colupulone and lupulone signals, 0.89 for the major adlupulone signal, 0.94 for humulone, 0.85 for cohumulone and adhumulone, 0.81–0.94 for the minor tautomers and 0.83–0.85 for W11 and W12 (medians over 49 samples). The integral of a window, however, also collects the tails of neighboring lines and any minor signal within it, and the two effects largely cancel in the sums used for quantitation: the summed fitted areas of the three principal α-acid lines were 0.985 (interquartile range 0.947–0.994) of the summed α-acid window integrals, and those of the six principal β-acid lines 0.93 of the six β-acid windows, the difference in the latter case arising chiefly from weak lines on the flanks of the major β-acid signals (at $\delta \approx 19.31$ and 19.23) that the windows include and the fit assigns separately. The effect of window truncation on the absolute contents is considered in Section A5.

A3.4 Statistical Assignment of the Minor Windows with 49 Samples

The regression of each minor window on the six major signals, which in v1.1 had been the only means of identifying the upfield integrals, was repeated with the 49 samples and the exact windows. Each window, expressed per 100 units of the six major signals so that the amount of extract cancels, was fitted by non-negative least squares without intercept, and the coefficients were bootstrapped over 2,000 resamplings (Table A2, Figure A3).

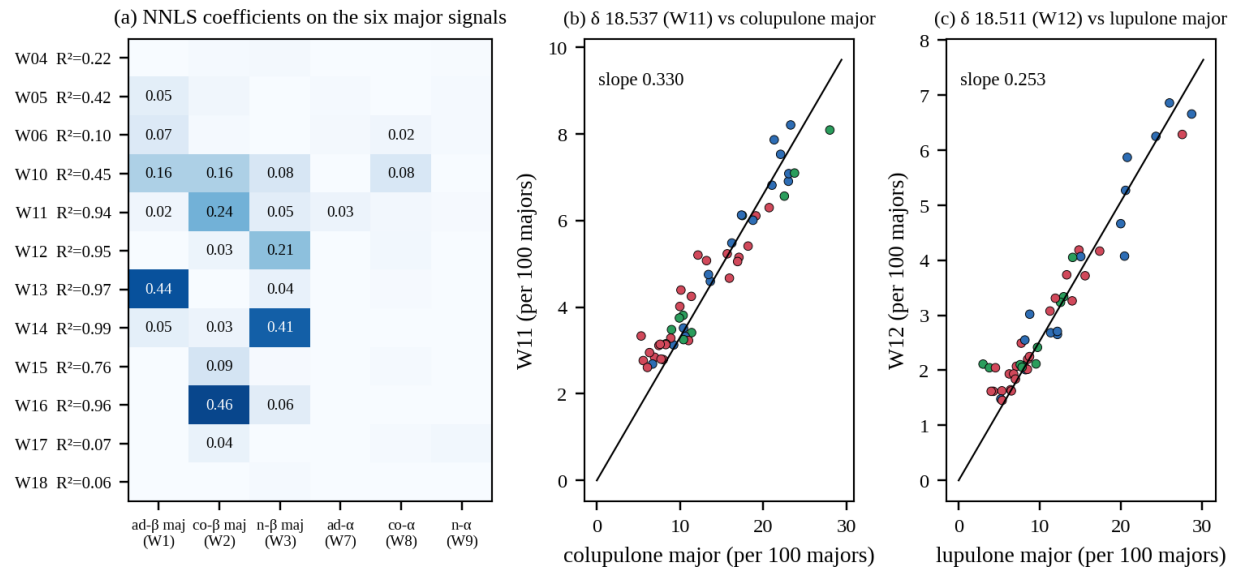

Figure A3. (a) Non-negative least-squares coefficients of each minor window on the six major hydroxyl signals (per 100 units of the six), with the coefficient of determination; coefficients below 0.02 are not printed. (b, c) The two β-associated signals at δ 18.537 and 18.511 against the major colupulone and lupulone signals, with lines through the origin; symbols are colored by region of growth.

The three minor tautomer windows are assigned without ambiguity. W13 (δ 18.403) is explained by adlupulone with a coefficient of 0.44 (95 % interval 0.34–0.52) and a small contribution from the tail of the adjacent lupulone line (0.04), W14 (δ 18.381) by lupulone (0.41, 0.36–0.44; $R^2 = 0.99$), and W16 (δ 18.294) by colupulone (0.46, 0.41–0.48) with a small lupulone contribution (0.06). The inference of v1.1, reached from the integral list alone and described there as probable but not proven, that the survey integral at δ 18.41 is the minor tautomer of adlupulone, is thereby confirmed, now from a separately resolved line of its own. The three coefficients, 0.44, 0.41 and 0.46, or 0.45 for lupulone when the part of its minor-tautomer line that falls in W13 is included, agree within their confidence intervals, and the ratio of the three minor to the three major signals, 0.494 (standard deviation 0.046) over the 49 samples, is homolog-independent, which confirms the withdrawal in v1.1 of the claim that the tautomeric equilibrium of colupulone differs from that of its homologs.

The pair at δ 18.537 and 18.511, the unassigned window of the Obercreek study and the seventh and eighth survey integrals of v1.1, is resolved as two homolog-specific signals: W11 is explained by colupulone (0.24, 0.20–0.27; $R^2 = 0.94$) and W12 by lupulone (0.21, 0.17–0.23; $R^2 = 0.95$), with negligible dependence on any α-acid. The adlupulone counterpart, which would be expected at about one quarter of the adlupulone major signal, is too small to be separated statistically and is presumably contained in one of the two windows. The weak signal W15 (δ 18.348) is also colupulone-associated (0.09, 0.06–0.10; $R^2 = 0.76$). The ratio of W11 plus W12 to the major β-acid signals is 0.285 (standard deviation 0.049) across the 49 samples, and it is the same in the older S1 samples (median 0.274), in the fresh S2 pellets (0.262), in the Cryo pellets (0.307) and in the ICE-4 extract (0.302). A signal that bears a fixed, homolog-specific proportion to each β-acid and does not change with the age of the material is not an oxidation product; it is either a third slowly exchanging form of the β-acids or a different compound formed in fixed proportion to each β-acid homolog. The ICE-4 test described in Section A3.5 bears on the choice between these alternatives.

The remaining windows are not bitter-acid tautomers. W4, W5, W6 and W17 are explained poorly by the six major signals ($R^2 = 0.07$–0.42), and the cluster W10 (δ 18.56–18.63) only moderately ($R^2 = 0.45$), with

contributions from both classes. These are independent chelated enols present at 1–10 % of the major signals, of which the cyclized and oxidized α-acid derivatives characterized by Li and co-workers, whose hydroxyl signals in $CDCl_3$ lie at δ 18.68 and 18.47–18.50, are plausible candidates for W10, which contains the first of these positions (the second falls within W12, where any contribution must be small, since W12 is explained almost entirely by lupulone),[6] and the 4-deoxy-α-acids (4-desoxyhumulones), which Shannon and co-workers determined alongside the α- and β-acid analogs by gas–liquid chromatography and NMR spectroscopy, are another;[7] no assignment is attempted here. The blank W18 is, as expected, unrelated to anything ($R^2 = 0.06$).

A3.5 The ICE-4 Test Proposed in Version 1.1

Version 1.1 proposed that the question of which upfield signals belong to the β-acids be settled with the ICE-4 calibration extract, whose certificate gives 10.98 % cohumulone, 31.60 % humulone plus adhumulone, 13.02 % colupulone and 13.52 % lupulone plus adlupulone, corresponding to a molar α/β ratio of 1.823. It was predicted that the ratio of the three α-acid signals to the three major β-acid signals would be close to 2.8 if only the minor tautomers belong to the β-acids and close to 3.4 if the δ 18.5 pair does as well. The spectrum recorded in the present campaign answers the question, although not in the way either prediction anticipated (Table A3).

Table A3. The ASBC ICE-4 calibration extract: certified values against the NMR results (spectrum Bryan-Hops-ICE4STD-H, recorded mass 95.4 mg, bottle not recorded).

Quantity	Certificate	NMR, composition	NMR, bottle A	NMR, bottle B
Total α-acids (% w/w)	42.58	—	10.38	22.85
Total β-acids (% w/w), major + minor tautomers	26.54	—	6.92	15.23
Recovery of the certified α-acids (%)	—	—	24.4	53.7
Recovery of the certified β-acids (%)	—	—	26.1	57.4
Cohumulone, mol % of α-acids	26.55	26.58		
Colupulone, mol % of β-acids (major + minor)	49.92	48.90		
α/β molar ratio, β = major signals only	—	2.603		
α/β molar ratio, β = major + minor tautomers	1.823	1.705		
α/β molar ratio, β = major + minor + W11 + W12	—	1.423		
Minor/major tautomer ratio	—	0.526		
(W11 + W12)/major β	—	0.302		

Certificate: cohumulone 10.98 %, humulone + adhumulone 31.60 %, colupulone 13.02 %, lupulone + adlupulone 13.52 % (w/w). Molar quantities from the certificate use the molar masses of Section A4.1, humulone and adhumulone being taken together. Version 1.1 predicted α/β (major signals only) ≈ 2.8 if only the minor tautomers belong to the β-acids and ≈ 3.4 if the δ 18.5 pair does as well.

The observed ratio of the α-acid signals to the major β-acid signals is 2.603. With the three minor tautomers counted as β-acid, the molar α/β ratio becomes 1.705, 6.5 % below the certificate; with W11 and W12 counted as well it becomes 1.423, 22 % below. The first rule is therefore the only one that is compatible with the certificate unless the α-acid hydroxyl signals are under-recovered relative to those of the β-acids by more than a fifth, and it is adopted in this addendum: β-acid contents are the sums of the major and minor tautomer windows, and W11 and W12 are reported separately. The residual deficit of 6.5 % is of the size, and in the direction, of the 9–12 % deficit of the α-acid 3-OH signal reported by Hoek and co-workers for isolated α-acids,[1] and of the exchange broadening of the α-acid lines noted above, and it is regarded as a measure of the accuracy of the α/β ratio from the hydroxyl region rather than as evidence against the

assignment. The homolog composition of ICE-4 agrees with the certificate closely: the cohumulone fraction of the α-acids is 26.58 mol % by NMR against 26.55 mol % calculated from the certificate, and the colupulone fraction of the β-acids 48.9 mol % against 49.9 mol %.

Taken together with the fixed, homolog-specific proportion of W11 and W12 to the β-acids, the ICE-4 result points toward a compound or form that accompanies each β-acid in constant proportion but is not measured as β-acid in the chromatographic assignment of the ICE-4 values. A third tautomer of the β-acids would not fit that description, since tautomers that interconvert in solution elute as one chromatographic peak; a biosynthetically related compound, such as the corresponding 4-deoxy-α-acid homolog, would,[7,8] but its hydroxyl shifts in $CDCl_3$ are not available to this study and the suggestion is untested. An exchange spectrum of purified β-acids, or spiking of a hop extract with a purified 4-deoxy-α-acid, would decide the matter.

A3.6 The Terpene Windows

The three olefinic windows carry the signals used for the hydrocarbon terpenes of hop oil by Farag and co-workers, the H-2 doublet of doublets of myrcene at δ 6.37 and the H-3 doublet of triplets of α-humulene at δ 5.61.[9] The myrcene window W19 contains the H-2 signal of every 2-substituted 1,3-diene in the oil, so that β-farnesene and (*E*)-β-ocimene are counted with myrcene; it is reported here as myrcene-equivalent content. The humulene signal is divided between W20 (δ 5.66–5.60) and W21 (δ 5.60–5.53), and in a pure humulene the ratio of the two halves would be constant. It is not: the ratio W20/W21 has a median of 0.65 but an interquartile range of 0.60–0.84 and values from below zero to 6.6, and both windows are negative in two low-oil samples, which shows that baseline curvature and at least one other signal contribute to W21. The humulene contents are therefore reported as the sum of the two windows, with the reservation that at contents below about 0.1 % they are not distinguishable from zero. β-Caryophyllene, whose trisubstituted olefinic proton gives the signal at δ 5.30 in the PNA spectrum of the commercial humulene isolate, does not interfere.

A4. Direct qNMR through a TMS-Transferred Dimethyl Sulfone Calibration

A4.1 Principle

In the classical internal-standard form of quantitative ^{1}H NMR, a weighed calibrant is dissolved in the same solution as the analyte, and the content follows from the ratio of the two integrals, the numbers of protons, the molar masses and the masses weighed, without calibration against the analyte itself.[10,11] The procedure used here separates the calibrant from the sample. The TMS contained in the deuterated solvent is present in both the calibration solution and the sample solution, and if the two are taken from the same bottle in the same volume, the TMS signal of each spectrum carries the same number of protons. Setting it to ten units in every spectrum places all the spectra on one scale, and a single calibration spectrum per bottle, in which a weighed quantity of DMS is dissolved in 800 µL of that bottle, converts the scale into moles. The approach belongs to the family of methods in which a signal of the solvent, rather than a weighed addition, serves as the concentration reference, whether it is the signal of a protonated solvent such as water[12] or the residual signal of a deuterated solvent,[13] and it shares with external calibration methods, of which PULCON and ERETIC are the best known,[14,15] the requirement that the link between calibration spectrum and sample spectrum be established rather than assumed. Its sequence is summarized in Figure A4.

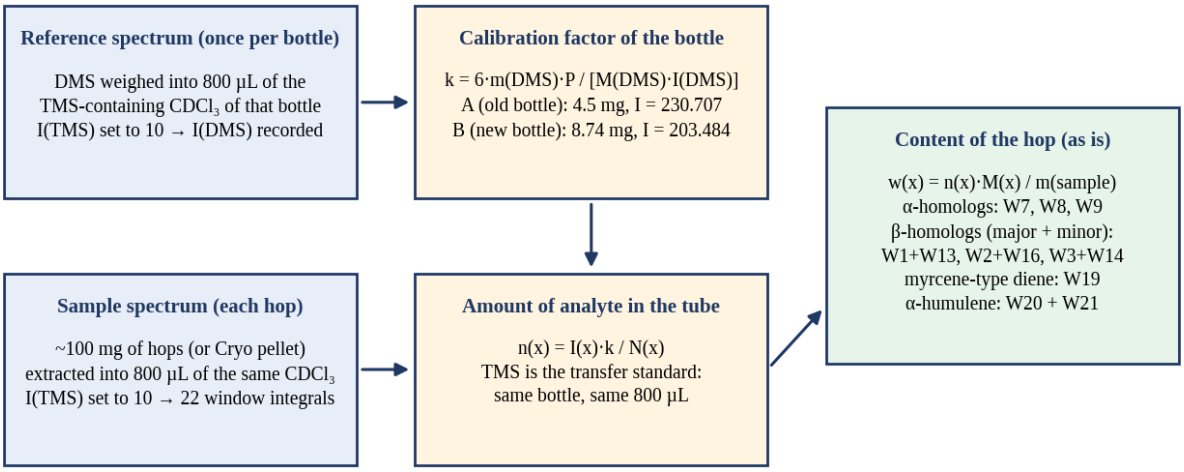

Figure A4. The TMS-transferred DMS calibration used for the direct qNMR of the 49 hop extracts. The TMS signal of each spectrum is set to ten units; the calibration factor of each bottle of $CDCl_3$ is obtained once from a solution of weighed DMS in 800 µL of that bottle.

For each bottle *s*, the calibration factor k_s, the number of millimoles of ^1H represented by one normalized integral unit, is obtained from the DMS spectrum:

$$k_s = N(DMS) \cdot m(DMS)_s \cdot P(DMS) / [M(DMS) \cdot I(DMS)_s] \quad (A1)$$

in which $N(DMS) = 6$ is the number of DMS protons, $m(DMS)_s$ the mass of DMS dissolved in 800 µL of the bottle, $P(DMS)$ its purity (0.9998), $M(DMS) = 94.128$ g mol^{-1} and $I(DMS)_s$ its integral with TMS equal to ten. For an analyte x whose signal of N_x protons has the normalized integral I_x in the spectrum of a hop extract of mass *m*, the amount in the tube and the content of the hop follow as

$$n_x = I_x \cdot k_s / N_x ; \quad w(x) = n_x \cdot M(x) / m \quad (A2)$$

which, written out in full, is the familiar internal-standard expression multiplied by the ratio of the solvent volumes in the sample and calibration tubes, a ratio taken as unity:

$$w(x) = [I_x / I(DMS)_s] \cdot [N(DMS) / N_x] \cdot [M(x) / M(DMS)] \cdot [m(DMS)_s / m] \cdot P(DMS) \cdot [V(sample) / V(DMS)] \quad (A3)$$

Every hydroxyl signal is a single proton ($N_x = 1$), as are the diene H-2 of myrcene and the H-3 of α-humulene. The α-acid homologs were calculated from W7, W8 and W9 with the molar masses of adhumulone and humulone (362.466 g mol^{-1}) and cohumulone (348.439), and the β-acid homologs from the sums of the major and minor tautomer windows, W1 + W13 (adlupulone, 414.586), W2 + W16 (colupulone, 400.559) and W3 + W14 (lupulone, 414.586), following Section A3.5. Myrcene-type diene was calculated as myrcene (136.238) and α-humulene with 204.357 g mol^{-1}. All contents are on the as-is basis, since no moisture determinations were made; the companion workbook performs every calculation with live formulas, so that the calibration constants can be edited.

A4.2 The Calibration of the Two Bottles

The two calibration spectra and the constants derived from them are given in Table A4. For the original bottle (A), 4.5 mg of DMS in 800 µL gave $I(DMS) = 230.707$, whence $k_A = 1.2431 \times 10^{-3}$ mmol per unit;

for the new bottle (B), 8.74 mg gave I(DMS) = 203.484 and k_B = 2.7373 × 10⁻³ mmol per unit. Because k = 12 n(TMS)/10, the same numbers give the TMS content of each bottle: 1.04 µmol in 800 µL (1.29 mM) for bottle A and 2.28 µmol (2.85 mM) for bottle B, a ratio of 2.20.

Table A4. Calibration of the two bottles of $CDCl_3$ (TMS) against dimethyl sulfone (800 µL; TMS integral set to 10): calibration factor k (Eq. A1) and the TMS content implied by it.

Bottle	DMS (mg)	I(DMS)	Windows: DMS; TMS (ppm)	k (mmol ^{1}H per unit)	TMS in 800 µL (µmol)	TMS (mM)	Samples
A (original bottle)	4.5	230.707	3.12–2.84; 0.03 to −0.05	1.2431 × 10⁻³	1.036	1.29	21 (S1)
B (new CIL bottle)	8.74	203.484	3.15–2.80; 0.05 to −0.08	2.7373 × 10⁻³	2.281	2.85	15 (S1) + 13 (S2)

k = 6·m(DMS)·P/[M(DMS)·I(DMS)], P = 0.9998, M(DMS) = 94.128 g mol⁻¹; n(TMS) = 10·k/12. Ratio k(B)/k(A) = 2.202. Nominal TMS contents of commercial $CDCl_3$: 0.03 % v/v ≈ 2.2 mM; 0.05 % v/v ≈ 3.7 mM.

The difference is the first important result of the addendum, because it shows that the TMS content of a bottle of $CDCl_3$ cannot be taken from its label. Commercial $CDCl_3$ is most commonly supplied with 0.03 or 0.05 % (v/v) of TMS, about 2.2 and 3.7 mM, and neither bottle contains a nominal amount. The TMS content of the older bottle is some 40 % below the lower of the two nominal grades and less than half that of the new bottle, a deficit that is most simply explained by the loss of TMS, which boils at about 27 °C, from a bottle that had been opened many times. The calibration spectrum of bottle A also shows a water signal at δ 1.59 far larger than that of bottle B, consistent with long use.[16] The practical corollary is that the calibration of a bottle is valid only for as long as its TMS content is stable, and that the TMS content of an opened bottle must be expected to fall with time. The date of the bottle A calibration relative to the extractions made with it is not recorded, and this is the largest unquantified uncertainty of the method (Section A5).

A4.3 Assignment of the Samples to the Bottles and the Test of the 8.74 mg Assumption

A wrong assignment of a sample to a bottle changes its results by the factor 2.20 and is therefore easy to detect by comparison with the declared α-acid content, even though the declared values are nominal. The test is summarized in Table A5 and in Figure A5.

Table A5. Test of the assignment of the samples to the two solvent bottles: ratio of the α-acid content by direct qNMR to the declared α-acid content under the assigned bottle and under the alternative.

Group	n	Bottle	Mean	Median	SD	Range	Alt. bottle	Mean (range) under alternative
S1 assigned to bottle A (incl. 022)	21	A	0.712	0.677	0.207	0.315–1.433	B	1.567 (0.693–3.156)
S1 assigned to bottle B	15	B	0.797	0.762	0.167	0.484–1.201	A	0.362 (0.220–0.545)
S2 pellets (043–050)	8	B	1.014	1.037	0.127	0.825–1.164	A	0.460 (0.375–0.529)
S2 Cryo pellets (038–042)	5	B	1.071	1.014	0.127	0.937–1.226	A	0.486 (0.426–0.557)
All S2 (038–050)	13	B	1.036	1.030	0.125	0.825–1.226	A	0.470 (0.375–0.557)
Sample 022 (duplicated 032 entry)	1	A	0.830				B	1.827

S2 under bottle B: r = 0.975 between measured and declared α-acids, slope 1.14, intercept −1.08 %, RMS difference 1.84 % α-acids. S1 bottle A vs bottle B: Welch t-test p = 0.18. S1 vs S2: Mann–Whitney p = 1 × 10⁻⁵.

For samples 038–050, the assumption that bottle B was used (8.74 mg of DMS) gives α-acid contents whose ratio to the declared values has a mean of 1.036, a median of 1.030, a standard deviation of 0.125 and a range of 0.825–1.226 over the thirteen samples. Under the alternative assumption of bottle A, the ratio would be 0.470 (0.375–0.557), that is, every one of these recently purchased samples, including Cryo pellets

sold on a certified analysis, would contain less than 56 % of its declared α-acids. The 8.74 mg assumption is therefore confirmed, the samples were retained in the quantitative analysis, and the instruction to withdraw them did not have to be applied. Across the thirteen samples the measured and declared α-acid contents are correlated with $r = 0.975$, a slope of 1.14 and an intercept of −1.08 % α-acids, and they differ by +0.76 % on average (standard deviation 1.74, root-mean-square difference 1.84 % α-acids).

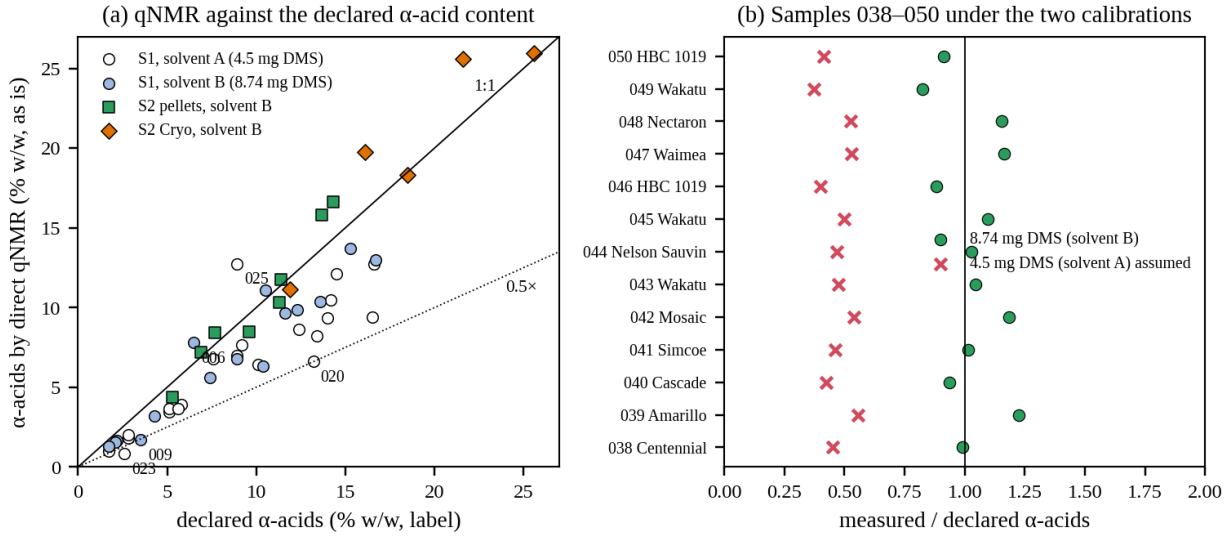

Figure A5. (a) α-Acid contents by direct qNMR against the α-acid contents declared on the packages, by sample set and solvent bottle; the solid line is the line of equality and the dotted line marks one half of the declared value. (b) Ratio of measured to declared α-acids for samples 038–050 under the two calibrations: bottle B (8.74 mg of DMS, adopted) and bottle A (4.5 mg).

For the S1 samples the assignments of the bottle workbook were tested in the same way. The 21 samples assigned to bottle A, including sample 022, whose entry had been duplicated as 032, gave a mean ratio of 0.712 (median 0.677; range 0.315–1.433), and the 15 assigned to bottle B a mean of 0.797 (median 0.762; range 0.484–1.201); the two groups do not differ significantly (Welch t-test, $p = 0.18$). Exchanging the bottles would raise the first group to 1.57 and lower the second to 0.36, and for sample 022 alone the ratio would become 1.83 against 0.83 as assigned. Every assignment of the workbook is thus consistent with the data, and 022 belongs to bottle A. The S1 samples as a whole, however, contain markedly less α-acid relative to their labels than the S2 samples (Mann–Whitney test, $p = 1 \times 10^{-5}$), about three quarters of the declared value on average.

That deficit is not a calibration artifact. It is found in both bottles; it is accompanied by an even larger deficit of hop oil, the median myrcene-type content being 0.31 % in S1 against 0.94 % in the S2 pellets; and losses of α-acids of this order during the storage of hops and pellets under non-ideal conditions are well documented, the loss being indexed by the hop storage index.[17,18] A declared α-acid content is, moreover, a nominal figure for a lot at the time of its analysis, commonly obtained by the spectrophotometric or conductometric methods, which read higher than HPLC because they include oxidation products,[19,20] and it says nothing about the history of the particular package. The S1 labels therefore cannot validate the absolute scale, and they are consistent with it only in the weaker sense that just three S1 samples exceed their declared values, Nelson Sauvin (008) by 6 %, Sterling (006) by 20 % and Belma (025) by 43 %.

The exception is sample 025 (Belma, declared 8.9 %), for which 12.75 % was found, 1.43 times the label, whereas the other Belma, 033, gave 6.77 %. The two carry the same label and the same recorded mass, and

their compositions differ: the α/β ratio is 3.56 in 025 and 2.41 in 033, and the cohumulone fraction 23.3 against 26.2 %. They are therefore not two spectra of one preparation, and either the label, the recorded mass or the bottle of 025 is in error; the sample should be re-weighed and re-run before its result is used.

A4.4 Results

The contents of the six homologs, the α- and β-acid totals, the ratios and the terpene contents of all 49 samples are given in Table A6, and the homolog contents are shown in Figure A6. The α-acid contents range from 0.82 % in the Savinjski Golding (023) to 25.96 % in the Cryo Simcoe (041), with a median of 8.23 %, and the β-acid contents from 1.09 % (023) to 13.48 % in the Cryo Cascade (040), with a median of 3.99 %. The molar α/β ratio spans more than a factor of ten, from 0.43 in the Hersbrucker (028) to 4.98 in the Bravo (016). The cohumulone fraction of the α-acids runs from 17.0 % in the Cryo Simcoe (18.0 % by line fitting) to 50.0 % in Vic Secret (57.4 % by line fitting, the fixed windows understating high cohumulone fractions for the reason given in Section A3.2), and the colupulone fraction of the β-acids from 37.0 % in Crystal to 74.7 % in Vic Secret. The myrcene-type diene ranges from 0.10 % to 2.83 % (Cryo Mosaic, 042) and α-humulene from indistinguishable from zero to 1.68 % (042).

Table A6. Direct qNMR results for the 49 samples (% w/w, as-is basis): α-acid homologs, β-acid homologs (major + minor tautomers), totals, molar α/β ratio, co-homolog fractions (mol %), myrcene-type diene (as myrcene), α-humulene, and the ratio of measured to declared α-acids.

Sample	Co-hum.	Hum.	Ad-hum.	Σα	Co-lup.	Lup.	Ad-lup.	Σβ	α/β	co-α %	co-β %	Myrc.	Hum-ene	α meas./decl.
001 Magnum	2.29	6.07	1.53	9.88	1.98	2.58	0.62	5.18	2.17	23.9	39.0	0.55	0.67	0.80
002 Galena	3.14	5.02	1.50	9.67	3.38	1.77	0.61	5.76	1.91	33.4	59.5	0.43	0.41	0.83
003 Vic Secret	4.61	3.18	1.63	9.42	3.56	0.80	0.45	4.81	2.23	50.0	74.7	0.16	0.45	0.57
004 Idaho 7	2.87	4.09	1.27	8.23	1.42	0.72	0.28	2.42	3.87	35.8	59.6	0.33	0.30	0.61
005 Ariana	2.45	3.03	0.86	6.34	2.46	1.32	0.31	4.09	1.76	39.6	61.0	0.16	0.22	0.61
006 Sterling	1.60	5.13	1.07	7.81	2.34	2.48	0.72	5.54	1.60	21.2	43.1	1.01	0.63	1.20
007 Summit	2.49	5.46	1.38	9.33	1.91	1.63	0.44	3.99	2.66	27.4	48.8	0.44	0.22	0.67
008 Nelson Sauvin	2.78	6.74	1.58	11.10	2.70	2.29	0.64	5.64	2.24	25.8	48.8	0.53	0.49	1.06
009 German (unsp.)	0.37	1.06	0.27	1.69	1.40	1.52	0.54	3.47	0.56	22.3	41.3	0.19	0.27	0.48
010 Waimea	2.72	7.72	1.71	12.14	2.08	1.96	0.52	4.55	3.03	23.1	46.5	0.76	0.24	0.84
011 Azacca	2.86	5.90	1.61	10.37	1.62	1.30	0.38	3.30	3.57	28.4	50.0	0.53	0.35	0.76
012 Crystal	0.39	1.03	0.23	1.65	1.13	1.60	0.38	3.12	0.60	24.2	37.0	0.26	0.16	0.75
013 Trad. German	0.92	1.92	0.59	3.43	1.07	0.91	0.34	2.32	1.69	27.4	47.0	0.19	0.12	0.67
014 Enigma	5.22	5.64	2.11	12.97	2.78	1.10	0.47	4.34	3.40	41.2	64.7	0.45	0.38	0.78
015 Sultana	2.36	4.77	1.49	8.61	1.16	0.91	0.31	2.38	4.11	28.1	49.6	0.67	0.43	0.69
016 Bravo	3.28	5.31	1.87	10.46	1.26	0.81	0.31	2.39	4.98	32.2	53.7	0.61	0.31	0.74
017 N. Brewer	1.38	1.92	0.63	3.93	1.54	0.72	0.27	2.54	1.76	36.1	61.6	0.17	< 0.1	0.68
018 Centennial	1.54	3.93	0.95	6.42	0.95	0.83	0.27	2.05	3.55	24.6	47.3	0.52	0.21	0.64
019 Saaz	0.40	1.07	0.33	1.81	0.98	1.12	0.41	2.51	0.82	22.9	40.0	0.13	< 0.1	0.65
020 Chinook	1.87	3.94	0.81	6.61	1.09	0.93	0.25	2.27	3.31	29.0	49.0	0.30	0.23	0.50
021 Spalt	0.39	0.92	0.26	1.57	1.10	1.06	0.35	2.51	0.71	25.5	44.5	0.16	< 0.1	0.75
022 Amarillo	1.60	5.25	0.78	7.63	1.94	2.63	0.46	5.03	1.73	21.6	39.4	0.55	0.39	0.83
023 Sav. Golding	0.27	0.44	0.10	0.82	0.56	0.38	0.15	1.09	0.85	34.2	52.5	0.10	0.15	0.31
024 Hallertau	0.44	1.27	0.32	2.03	1.05	1.19	0.38	2.61	0.88	22.3	40.8	0.18	0.20	0.73
025 Belma	2.88	7.87	2.00	12.75	1.91	1.62	0.55	4.07	3.56	23.3	47.8	0.35	0.45	1.43
026 Magnum	1.84	4.14	1.02	7.00	1.55	1.23	0.38	3.16	2.52	27.0	49.8	0.35	0.20	0.79
027 Cluster	1.85	2.86	0.88	5.59	2.15	1.15	0.41	3.71	1.71	33.9	58.7	0.25	< 0.1	0.76
028 Hersbrucker	0.20	0.63	0.15	0.98	0.98	1.21	0.41	2.60	0.43	21.2	38.4	0.20	0.18	0.58
029 Perle	1.13	1.89	0.63	3.66	1.08	0.67	0.30	2.06	2.02	31.7	53.5	0.24	0.31	0.72
030 Hall. Blanc	1.60	4.26	0.92	6.78	1.56	1.82	0.46	3.83	2.02	24.3	41.5	0.25	< 0.1	0.89

Sample	Co-hum.	Hum.	Ad-hum.	Σα	Co-lup.	Lup.	Ad-lup.	Σβ	α/β	co-α %	co-β %	Myrc.	Hum-ene	α meas./decl.
031 Herkules	3.88	6.98	1.88	12.75	1.60	1.24	0.36	3.19	4.55	31.3	50.9	0.59	0.50	0.77
032 Cascade	1.12	2.04	0.48	3.64	1.75	1.50	0.37	3.62	1.15	31.5	49.2	0.34	< 0.1	0.65
033 Belma	1.72	4.07	0.97	6.77	1.55	1.21	0.43	3.19	2.41	26.2	49.4	0.24	0.29	0.76
034 Hersbrucker	0.26	0.84	0.22	1.31	1.11	1.29	0.42	2.82	0.53	20.3	40.2	0.14	0.21	0.77
035 Nugget	3.18	8.58	1.96	13.71	1.54	1.29	0.45	3.28	4.75	23.9	47.8	0.72	0.49	0.90
036 Huell Melon	0.83	1.85	0.49	3.18	2.54	2.21	0.61	5.36	0.67	26.9	48.3	0.24	0.10	0.74
038 Centennial	3.93	11.42	2.98	18.33	2.84	2.52	0.78	6.13	3.39	22.1	47.1	2.51	1.24	0.99
039 Amarillo	3.87	12.96	2.90	19.73	5.23	6.28	1.34	12.85	1.75	20.3	41.5	2.04	1.67	1.23
040 Cascade	3.10	6.43	1.63	11.15	6.62	5.52	1.34	13.48	0.94	28.6	50.0	1.81	0.99	0.94
041 Simcoe	4.27	18.21	3.48	25.96	2.84	3.44	0.88	7.16	4.12	17.0	40.5	1.38	1.40	1.01
042 Mosaic	4.90	15.59	5.12	25.62	2.99	2.60	0.95	6.54	4.44	19.8	46.6	2.83	1.68	1.19
043 Wakatu	2.20	3.90	1.11	7.20	4.83	2.71	1.04	8.57	0.95	31.3	57.2	0.93	0.45	1.04
044 Nelson Sauvin	2.65	7.56	1.53	11.74	2.64	2.46	0.64	5.74	2.32	23.3	46.8	0.82	0.77	1.03
045 Wakatu	2.52	4.61	1.32	8.44	5.17	2.94	1.05	9.15	1.05	30.6	57.3	1.07	0.52	1.10
046 HBC 1019	1.76	5.48	1.25	8.48	2.65	2.38	0.92	5.95	1.62	21.4	45.5	0.66	0.60	0.88
047 Waimea	4.30	9.85	2.50	16.65	3.45	2.64	0.78	6.87	2.75	26.6	51.1	1.40	0.81	1.16
048 Nectaron	4.06	9.32	2.45	15.82	2.92	2.52	0.70	6.14	2.93	26.4	48.4	1.19	1.15	1.16
049 Wakatu	1.36	2.32	0.69	4.37	3.88	2.03	0.79	6.70	0.74	32.0	58.8	0.47	0.56	0.82
050 HBC 1019	2.45	6.26	1.60	10.31	3.90	2.81	1.09	7.79	1.50	24.5	50.9	0.94	0.74	0.91

Provisional absolute scale (Section A5): contents carry an estimated uncertainty of about ±10 %; ratios and homolog fractions do not depend on the calibration. Line fitting indicates that the fixed windows overstate the adhumulone fraction of the Cryo pellets (038–042) by 3.7–5.0 points and understate their cohumulone fraction by 1.0–4.8 points, and understate the cohumulone fraction of the high-cohumulone pellets 003, 005 and 014 by 4.4–7.4 points (Section A3.2). Hum-ene: α-humulene; values below 0.1 % are not distinguishable from zero. Sample 025: see Section A4.3.

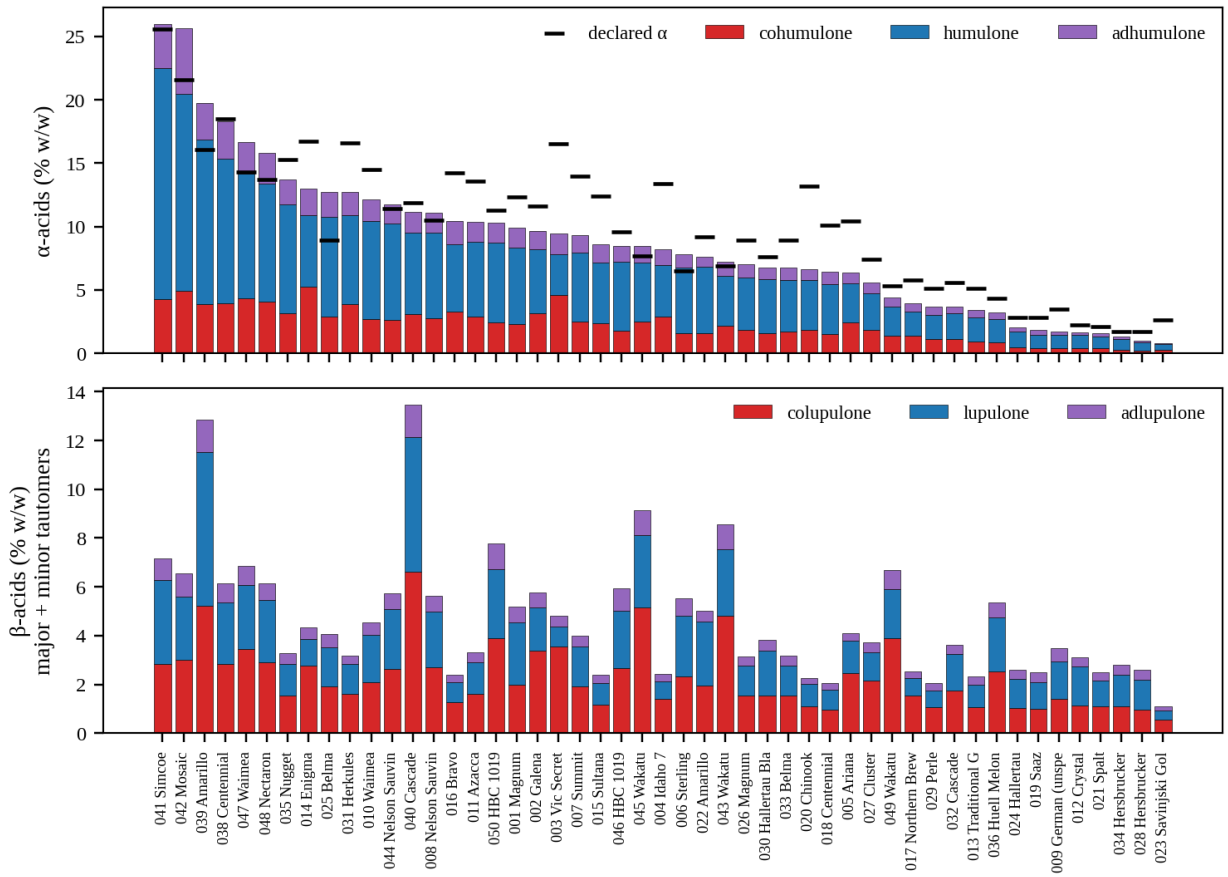

Figure A6. Contents of the three α-acid homologs (upper) and of the three β-acid homologs, major plus minor tautomers (lower), in the 49 hop samples by direct qNMR (% w/w, as is), ordered by total α-acids; bars mark the declared α-acid content.

The Cryo pellets contained 2.6–3.1 times the α-acids, 2.6–3.7 times the β-acids and 3.7–5.4 times the myrcene-type diene of the retail pellets of the same cultivars in S1, whereas their declared α-acid contents were only 1.75–2.12 times higher. The enrichment of about twofold that the process is designed to give[5] accounts for the declared ratios, and the larger measured ratios reflect the lower contents of the older S1 pellets, in the essential oil above all, rather than any excess in the Cryo products, whose ratio to the declared value is 1.07 on average. Their composition, on the other hand, is that of the parent cultivar: the α/β ratios of the Cryo and retail pellets are 3.39 and 3.55 for Centennial, 1.75 and 1.73 for Amarillo and 0.94 and 1.15 for Cascade.

A4.5 The ICE-4 Extract as an Absolute Check

The ICE-4 extract should have provided the one absolute validation of the procedure, and it did not (Table A3). With the recorded mass of 95.4 mg, bottle B gives 22.85 % α-acids and 15.23 % β-acids, 54 % and 57 % of the certified values, and bottle A 10.38 % and 6.92 %, 24 % and 26 %. Neither agrees. Degradation of the reference material cannot be excluded, but it is not suggested by the spectrum: the homolog composition matches the certificate to within one percentage point, the molar α/β ratio is within 7 % of it, and the oxidation-sensitive cluster W10 is no larger relative to the α-acids (0.049) than in the hops. The two recording irregularities noted in Section A2.4 are the more probable explanations: the ICE-4 spectrum is assigned to neither bottle, and its printed mass is that of sample 026. A mass of 51–55 mg with bottle B

would reproduce both certified values within about 7 %, but that is conjecture. The result has to be recorded as a failed check, and the repetition of the ICE-4 measurement with a documented mass and a DMS calibrant added directly to the tube is the most valuable single experiment that remains to be done.

A4.6 Same-Cultivar Comparisons

Ten cultivars are represented more than once, and their comparisons, given in Table A7, separate what is fixed by the genotype from what is not. The clearest case is Wakatu, of which three harvests were examined. The α-acid content was 4.37 % in the 2022 sample, 7.20 % in 2023 and 8.44 % in 2024, in the same order as the declared values (5.3, 6.9 and 7.7 %), and the α/β ratio rose from 0.74 to 1.05, whereas the cohumulone fraction (32.0, 31.3 and 30.6 %) and the colupulone fraction (58.8, 57.2 and 57.3 %) varied by little more than a percentage point. The homolog distributions of a cultivar are thus reproduced across harvests within the uncertainty of the windows, as Molyneux and Wong concluded from eight Cascade lots in 1975,[4] while the amounts and the α/β ratio depend on the lot and its age; the lower α/β ratio of the oldest Wakatu may reflect lot-to-lot variation or a preferential loss of α-acids on storage, and three samples cannot distinguish the two. The two HBC 1019 samples (2022 and 2024) differ by 3.1 points in cohumulone and by 5.4 points in colupulone (45.5 against 50.9 %), and the retail and 2023 Waimea samples by 3.5 and 4.6 points, differences several times larger than those among the three Wakatu harvests whose cause a single pair of samples cannot establish. The retail and 2023 Nelson Sauvin samples are nearly indistinguishable (α-acids 11.10 and 11.74 %, α/β 2.24 and 2.32), as are the two Hersbrucker samples in composition.

Two pairs do not behave as replicate samples of one cultivar should. The Belma pair has been discussed above. The Magnum pair differs by 10.7 points in its colupulone fraction (39.0 % in the German Magnum, 001, and 49.8 % in 026), a difference far outside the within-cultivar range of the other pairs; the composition of 026 is, on the other hand, almost identical to that of the Belma 033 (cohumulone 27.0 and 26.2 %, colupulone 49.8 and 49.4 %, α/β 2.52 and 2.41), which strengthens the suspicion expressed in v1.1 that its label, which carries the Belma value of 8.9 %, was transcribed from the neighboring sample. Both questions should be resolved from the laboratory records before the samples are used as references.

Table A7. Cultivars represented by more than one sample: declared and measured α-acids, β-acids, α/β, co-homolog fractions and myrcene-type diene, and the distance between the two samples in the first three principal components of the compositional data set (as a fraction of the median distance between all pairs) with the rank of the partner among the nearest neighbors.

Cultivar	Samples	Forms	Declared α (%)	α (%)	β (%)	α/β	co-α (%)	co-β (%)	Myrcene (%)	Distance / median	Rank
Magnum	001 / 026	Pellet / Pellet	12.3 / 8.9	9.88 / 7.00	5.18 / 3.16	2.17 / 2.52	23.9 / 27.0	39.0 / 49.8	0.55 / 0.35	0.31	4
Nelson Sauvin	008 / 044	Pellet / Pellet	10.5 / 11.4	11.10 / 11.74	5.64 / 5.74	2.24 / 2.32	25.8 / 23.3	48.8 / 46.8	0.53 / 0.82	0.35	9
Waimea	010 / 047	Pellet / Pellet	14.5 / 14.3	12.14 / 16.65	4.55 / 6.87	3.03 / 2.75	23.1 / 26.6	46.5 / 51.1	0.76 / 1.40	0.42	13
Centennial	018 / 038	Pellet / Cryo	10.1 / 18.5	6.42 / 18.33	2.05 / 6.13	3.55 / 3.39	24.6 / 22.1	47.3 / 47.1	0.52 / 2.51	0.69	20
Amarillo	022 / 039	Pellet / Cryo	9.2 / 16.1	7.63 / 19.73	5.03 / 12.85	1.73 / 1.75	21.6 / 20.3	39.4 / 41.5	0.55 / 2.04	0.36	3
Belma	025 / 033	Pellet / Pellet	8.9 / 8.9	12.75 / 6.77	4.07 / 3.19	3.56 / 2.41	23.3 / 26.2	47.8 / 49.4	0.35 / 0.24	0.35	7
Hersbrucker	028 / 034	Pellet / Pellet	1.7 / 1.7	0.98 / 1.31	2.60 / 2.82	0.43 / 0.53	21.2 / 20.3	38.4 / 40.2	0.20 / 0.14	0.30	1
Cascade	032 / 040	Pellet / Cryo	5.6 / 11.9	3.64 / 11.15	3.62 / 13.48	1.15 / 0.94	31.5 / 28.6	49.2 / 50.0	0.34 / 1.81	0.78	18
Wakatu	043 / 045	Pellet / Pellet	6.9 / 7.7	7.20 / 8.44	8.57 / 9.15	0.95 / 1.05	31.3 / 30.6	57.2 / 57.3	0.93 / 1.07	0.12	1
Wakatu	043 / 049	Pellet / Pellet	6.9 / 5.3	7.20 / 4.37	8.57 / 6.70	0.95 / 0.74	31.3 / 32.0	57.2 / 58.8	0.93 / 0.47	0.46	4

Cultivar	Samples	Forms	Declared α (%)	α (%)	β (%)	α/β	co-α (%)	co-β (%)	Myrcene (%)	Distance / median	Rank
Wakatu	045 / 049	Pellet / Pellet	7.7 / 5.3	8.44 / 4.37	9.15 / 6.70	1.05 / 0.74	30.6 / 32.0	57.3 / 58.8	1.07 / 0.47	0.58	7
HBC 1019	046 / 050	Pellet / Pellet	9.6 / 11.3	8.48 / 10.31	5.95 / 7.79	1.62 / 1.50	21.4 / 24.5	45.5 / 50.9	0.66 / 0.94	0.19	1

Wakatu: 043 (2023), 045 (2024), 049 (2022). HBC 1019: 046 (2022), 050 (2024). Nelson Sauvin 044 and Waimea 047: 2023. Rank 1 = the partner is the nearest neighbor among the other 48 samples.

A4.7 The Co-Homolog Relationship

The linear relationship between the colupulone fraction of the β-acids and the cohumulone fraction of the α-acids reported in v1.1 for the 36 survey samples (slope 1.33, intercept 11.6 percentage points, $r^2 = 0.90$) is reproduced exactly by the S1 samples of the present data set (slope 1.327, intercept 11.56, $r^2 = 0.897$), which confirms that the major windows used here are those of the v1.1 archive. With all 49 samples the slope is 1.23, the intercept 15.4 and r^2 0.84 (Figure A7). Part of the reduction is caused by the Cryo pellets, whose cohumulone fractions are understated by the fixed windows (Section A3.2); with their line-fit values the slope becomes 1.27 and r^2 0.86. The three Wakatu samples lie three to four points above the line, with colupulone fractions of 57–59 % at cohumulone fractions of 31–32 %, and the German Magnum (001), the retail Cascade (032) and Crystal (012) lie five to nine points below it; the relationship is therefore a useful consistency check but not a tight one across genetically diverse cultivars.

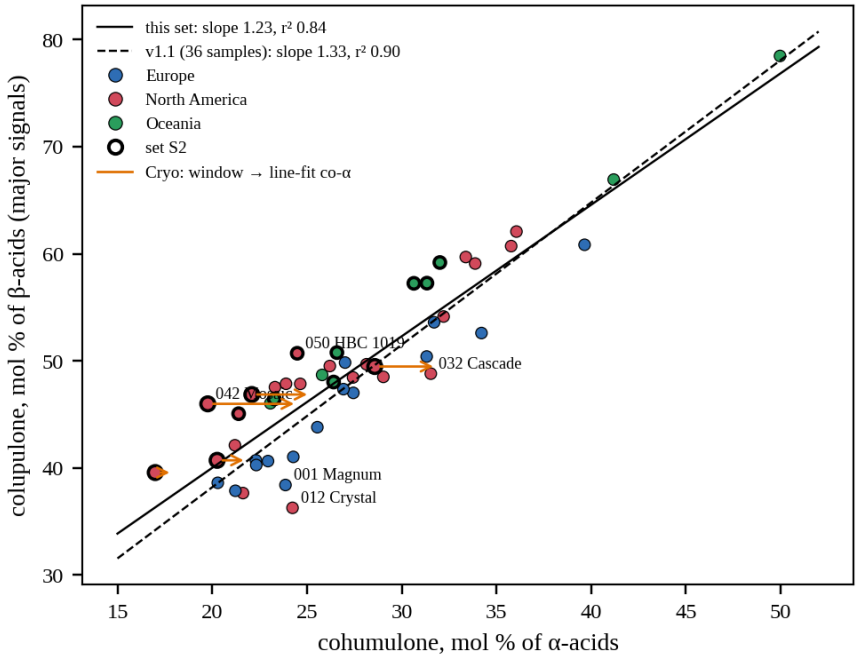

Figure A7. Colupulone fraction of the β-acids (major tautomer signals) against the cohumulone fraction of the α-acids for the 49 samples, with the regression line of this data set and that of v1.1. Heavy outlines mark set S2; arrows show the shift of the Cryo pellets when their cohumulone fractions are taken from line fitting instead of the fixed windows.

A4.8 Terpenes

The myrcene-type diene and α-humulene contents follow the product and its age more closely than the cultivar. The median myrcene-type content is 0.31 % in S1, 0.94 % in the fresh S2 pellets and 2.04 % in the Cryo pellets, and α-humulene 0.24, 0.67 and 1.40 % respectively. Both are hydrocarbons that are lost from hops by evaporation and oxidation during storage, and both can be lost from the sample during

extraction, so that the NMR values are lower bounds to the contents of the hop as sampled. The humulene values carry the additional uncertainty described in Section A3.6. Within these limits the ratio of the myrcene-type signal to the α-acids, which rises from 0.15 in S1 to 0.23 in the S2 pellets and 0.29 in the Cryo pellets (medians), is a useful index of freshness, and it is this ratio, rather than any geographic property, that drives the oil-related dimension of the chemometric models of Section A8.

A5. Uncertainty of the Calibration Route and Audit of the Method

The components of uncertainty that can be estimated from the data are listed in Table A8, together with those that cannot. The estimates are relative standard uncertainties of a single α- or β-acid content and are given separately for the two bottles.

Table A8. Uncertainty budget of the α- and β-acid contents obtained through the TMS-transferred DMS calibration (relative standard uncertainties, %).

Component	Bottle A	Bottle B	Type / direction	Basis of the estimate
Mass of hop sample	0.05	0.05	random	S1 masses recorded to 0.1 mg, S2 to 0.01 mg, ~100 mg samples; balance repeatability ~0.02 mg assumed.
Mass of DMS in the reference solution	0.68	0.12	random (per bottle, systematic for all samples in that bottle)	A: "4.5 mg" recorded to two significant figures (±0.05 mg rounding, rectangular) plus 0.01 mg balance; B: 8.74 mg.
Purity of DMS	0.10	0.10	systematic	Taken as 0.9998 from the PNA terpene-assay worksheet; certificate not part of this data set.
Solvent volume, sample tube vs reference tube (800 µL each)	1.40	1.40	random	Assumed 1 % repeatability per delivery of $CDCl_3$ with the same pipette; a common delivery bias cancels.
Relaxation (d1 = 15 s; pulse angle and acquisition time not recorded)	1.00	1.00	systematic, sign uncertain	DMS T_1 4–5 s in $CDCl_3$ (BIPM ISRD-02); α-acid 3-OH T_1 about 4 s; TMS saturation cancels only if T_1(TMS) is the same in reference and sample.
Integration: TMS window 0.24 ppm (samples) vs 0.085/0.134 ppm (references)	2.70	1.40	systematic, analyte LOW	Lorentzian TMS lines (1.5/1.9 Hz) in the reference spectra are integrated over narrower windows; estimated from the digitized reference traces.
Integration: DMS ^{13}C satellites outside the DMS window	1.10	1.10	systematic, analyte HIGH	1.07 % of DMS intensity lies in satellites at δ 2.75 and 3.21 (outside the window); hydroxyl signals have no satellites.
Integration: truncation of analyte lines vs inclusion of minor lines	1.50	1.50	systematic, small	Line fitting of the digitized spectra: Σ fitted α lines / Σ α windows median 0.985 (IQR 0.947–0.994); for β 0.93, because the β windows also collect minor lines.
Loss of TMS (volatility) between reference and sample preparation	not quantified	not quantified	systematic, sign depends on history	Not quantifiable from the data. Bottle A contained 1.29 mM TMS against 2.85 mM in the new bottle B, consistent with loss of TMS from an opened bottle; loss from a sample tube during extraction biases results HIGH.
H/D exchange and exchange broadening of the enolic OH	not quantified	not quantified	systematic, analyte LOW	Hoek et al. found the α-acid 3-OH 9–12 % below the prenyl signals (possibly relaxation). ICE-4: NMR α/β 6.5 % below the certificate.
Completeness of a single 800 µL extraction	not quantified	not quantified	systematic, analyte LOW	Never verified by re-extraction.
Combined (quantified components only), relative standard uncertainty	3.77	2.90		Root-sum-square of the quantified random and systematic terms above; see text.

The combined figure includes only the quantified components. The three unquantified components can each exceed it; the empirical comparison with the declared α-acid contents and the failed ICE-4 check are discussed in Sections A4.3–A4.5.

The weighing of the hop sample contributes negligibly. The mass of DMS in the calibration solution of bottle A, recorded as 4.5 mg with two significant figures, contributes 0.7 %, almost entirely through its rounding, against 0.1 % for the 8.74 mg of bottle B, and a larger weighed mass recorded to 0.01 mg would remove the term. The purity of the DMS was taken as 0.9998, the value entered in the PNA terpene-assay worksheet; dimethyl sulfone is well established as a qNMR calibrant and is the subject of a BIPM internal-standard reference data sheet, which gives its longitudinal relaxation time in $CDCl_3$ as 4–5 s and its

solubility as greater than 5 mg mL^{-1}.[21–23] The bottle B solution, at 10.9 mg mL^{-1}, is above that figure, and the complete dissolution of the calibrant should be confirmed visually in any repetition. The volumes of the calibration and sample solutions enter as a ratio and were assumed to be equal; a repeatability of 1 % per delivery of a dense, volatile solvent by pipette gives 1.4 % for the ratio, while a common bias of the pipette cancels.

The relaxation conditions are only partly known. With a 15 s relaxation delay, DMS (T_1 4–5 s) and the enolic protons (T_1 about 4 s for the α-acid 3-OH[1]) are fully relaxed at small pulse angles and relaxed to about 97–98 % at 90°, depending on the acquisition time, which was not recorded; TMS relaxes more slowly, but its saturation cancels provided that its T_1 is the same in the calibration and sample solutions, which is plausible but has not been checked. A standard uncertainty of 1 % has been assigned. Three integration effects were quantified from the digitized spectra. The TMS signal was integrated over δ 0.12 to −0.12 in the sample spectra but over narrower windows in the two calibration spectra (0.085 and 0.134 ppm), which, for the Lorentzian TMS lines of 1.5–1.9 Hz observed there, capture 1.4–2.7 % less of the line and bias the analyte results low by that amount. The DMS window excludes the ^{13}C satellites of DMS at δ 2.75 and 3.21 (1.07 % of its intensity), whereas the hydroxyl signals have none, and it truncates the wings of the DMS line by a further 0.8 %, so that the DMS integral is 1.8 % low and the results correspondingly high. The truncation of the analyte lines by their windows and the inclusion of neighboring minor lines nearly cancel (Section A3.3); referred to the fitted principal lines, the α-acid window integrals are 1.5 % high. Treated as corrections, the three effects would change the α-acid contents by −0.7 % in bottle A and −2.0 % in bottle B, which is within the uncertainty; they have not been applied. The root-sum-square of the quantified components is 3.8 % for bottle A and 2.9 % for bottle B.

Three further components could not be quantified, and any one of them may exceed the combined figure. The first and most serious is the stability of the TMS content. The transfer standard is volatile, bottle A contains less than half the TMS of bottle B, most probably because TMS has been lost from the opened bottle, and neither the interval between the calibration and the extractions nor the time for which the extraction vials stood open, were sonicated or were filtered is recorded; TMS lost from a sample tube before acquisition biases that result high, and TMS lost from the bottle between extraction and calibration biases all results from that bottle low. The second is exchange of the enolic protons with the deuterium of the solvent and its impurities, which can only lower the hydroxyl integrals and which the ICE-4 α/β ratio bounds at about 7 % for the α-acids relative to the β-acids. The third is the completeness of a single extraction of 100 mg of hops into 800 µL of $CDCl_3$, which has never been tested by re-extraction and can only lower the results.

The empirical evidence is consistent with a combined uncertainty of the order of 5–10 %. The thirteen S2 samples agree with their declared α-acid contents with a root-mean-square difference of 1.84 % α-acids and a standard deviation of the ratio of 12.5 %, but that spread includes the uncertainty of the declared values, whose method and date are unknown, and cannot be apportioned. The failure of the ICE-4 check (Section A4.5) removes the one independent test of the absolute scale, and until it has been repeated, the absolute contents reported here should be regarded as provisional to within about ±10 %, the relative quantities, homolog fractions and α/β ratios as well founded, and the comparison of samples measured with the same bottle as more reliable than a comparison across bottles.

A6. Design of the Chemometric Analysis

A6.1 Two Views of One Measurement

The chemometric analysis was carried out on two views of the same spectra, as requested: the integrals as recorded, and the chemically identified components derived from them. Each view was examined in two forms, one carrying the absolute scale that the TMS transfer now provides and one carrying composition only, because the amount of extract and its composition answer different questions and are confounded in different ways.

The integral data set, I_abs, contains the 21 sample windows W1–W21 of every spectrum expressed in millimoles of ^{1}H per kilogram of hop, that is, each normalized integral multiplied by the calibration factor of its bottle and divided by the sample mass. The TMS window W22 was excluded because it is equal to ten in every spectrum by construction, carries no information about the sample and would, if expressed per kilogram, reproduce only the bottle and the mass; the blank window W18 was retained deliberately as a control for noise and baseline artifacts. The compositional form, I_rel, expresses the same 21 windows per 100 units of the six major bitter-acid signals, the convention of v1.1, from which the amount of extract cancels. The component data set, Q_abs, contains the eight quantified constituents in % w/w, the three α-acid homologs, the three β-acid homologs (major plus minor tautomers), the myrcene-type diene and α-humulene, and Q_rel the same eight constituents as percentages of their sum. Negative humulene values were set to zero in Q_rel only, and the signals of Section A3.4 that are not bitter-acid tautomers, which are present in the integral data, have no counterpart in the component data. The four matrices are given in the companion workbook.

A6.2 Pretreatments

Pretreatment was treated as a question to be answered by the data rather than as a convention, as requested, although the PNA convention of mean-centering followed by Pareto scaling was taken as the reference. Six column scalings were compared, mean-centering alone (MC), autoscaling to unit variance (UV), Pareto scaling (division by the square root of the standard deviation), range scaling, level scaling (division by the mean) and variable stability (VAST) scaling (autoscaling multiplied by the inverse coefficient of variation),[24–26] each without transformation, after a generalized logarithm with the transformation parameter set to the noise variance estimated from the blank window,[27] and, for the component data, after the centered log-ratio transformation of compositional data analysis.[28] Sixty combinations were evaluated in all.

Four criteria were used, none of which depends on the grouping that the analysis is meant to discover. The first is noise leverage, measured as the share of the total variance after pretreatment carried by the blank window W18; a pretreatment that gives a window containing no signal a large share of the variance will generate structure from noise. The second is the recovery of same-cultivar similarity, measured as the rank of the nearest sample of the same cultivar among the 48 others, for the seven cultivars represented by two or three samples in the same product form, and separately for the three pellet–Cryo pairs. The third is the separation of known classes, by silhouette width in the space of the first three principal components and by the balanced accuracy of a three-nearest-neighbor classifier under leave-one-cultivar-out validation with the pretreatment refitted in every fold. The fourth is an artifact check, the silhouette of the two solvent bottles among the S1 pellets, which should be close to zero.

A6.3 Methods

The unsupervised methods were PCA, with the number of components judged by element-wise *k*-fold cross-validation (Q^2),[29] the broken-stick rule and parallel analysis,[30] and with Hotelling T^2 and the residual Q statistic with the limits of Jackson and Mudholkar;[31,32] hierarchical cluster analysis by Ward's criterion on Euclidean distances,[33] with the number of clusters guided by the silhouette width,[34] the stability of each cluster measured by the mean Jaccard coefficient over 200 bootstrap resamplings[35] and the agreement between partitions by the adjusted Rand index;[36] *k*-means clustering as a check on the Ward partitions; and UMAP[37] (8 neighbors, minimum distance 0.3) and *t*-SNE[38] (perplexity 8, principal-component initialization) in two and three dimensions. The faithfulness of each low-dimensional map was measured by its trustworthiness,[39] by the fraction of each sample's five nearest neighbors in the full pretreated data that remain among its five nearest neighbors in the map, and, for UMAP and *t*-SNE, by the agreement of the neighborhoods obtained with ten different random seeds, since both methods are known to distort global distances and to create apparent clusters.[40,41]

The supervised methods were PLS-DA,[42,43] support vector machines with linear and radial-basis kernels,[44] linear discriminant analysis with Ledoit–Wolf shrinkage of the covariance matrix,[45] *k*-nearest neighbors, L2-regularized multinomial logistic regression, random forests[46] and SIMCA class modeling,[47] in which one principal component model is built for each class and a sample is assigned to the class to whose model it is nearest in the combined T^2–Q distance. Four targets were modeled: the region of growth and the region in which the cultivar was bred (three classes each), the product form (Cryo or pellet), included as a positive control that should be easy on absolute data and hard on compositional data, and the trade classification of the cultivar as aroma, dual-purpose or bittering. Every model was assessed by leave-one-cultivar-out cross-validation, in which all samples of a cultivar are withheld together, so that the ten cultivars represented more than once cannot inform their own predictions; the 38 outer folds contained a grouped four-fold inner cross-validation in which the hyperparameters were tuned, and the pretreatment (mean-centering and Pareto scaling) was fitted on the training samples of each fold.[48–50] Balanced accuracy, the mean of the class-wise recoveries, was used as the figure of merit because the classes are unequal in size; its chance level is 0.33 for three classes and 0.50 for two.

Significance was established by permutation. The class labels were permuted among cultivars, so that all samples of a cultivar kept a common label, and the entire nested procedure was repeated for each permutation, 100 times for PLS-DA on all four data sets and 50 times for the radial-basis SVM on the two integral data sets (100 times for the region of growth on I_abs); because the best of several models is an optimistic estimate, a further test permuted the labels and recorded, for each permutation, the best of five models (PLS-DA, LDA, *k*-nearest neighbors, logistic regression and SIMCA), 50 times. Baselines were computed with the same validation: the majority class, a model using the declared α-acid content alone, and models using only three chemical descriptors, the logarithm of the α/β ratio and the cohumulone and colupulone fractions, or only the first two of these; each baseline model was fitted by logistic regression, the radial-basis SVM and shrinkage LDA, and the best of the three is reported. Finally, two confounding checks were made: the prediction of the measurement set (S1 or S2) among the pellets and of the solvent bottle within S1, which ought to fail if the data are free of campaign artifacts, and the prediction of the geographic targets within S1 alone and within the pellets alone. The calculations were made in Python 3.11 with NumPy 2.4, SciPy 1.17, scikit-learn 1.8[51] and umap-learn 0.5, with all random seeds fixed.

A7. Choice of Pretreatment

The comparison of pretreatments is summarized in Table A9 for the untransformed data and in the companion workbook for all sixty combinations, and its most instructive case is illustrated in Figure A8. Three pretreatments can be set aside at once.

Level scaling, which divides each variable by its mean, gave the blank window 55 % of the total variance of I_abs and 87 % of that of I_rel, because the mean of a window that contains no signal is close to zero; after the generalized logarithm the share rose to 91 %. The first principal component of I_abs after level scaling is therefore the blank, and because the blank carries a small baseline offset in the S2 spectra (Section A2.4), that component separates the two measurement campaigns cleanly (Figure A8, right). Any conclusion drawn from such a map about the samples of S2, which include six of the ten Oceania samples and all five Cryo pellets, would be an artifact of baseline processing. Unit-variance and range scaling are less extreme but share the defect in principle, since they give the blank 4.8–6.6 % of the variance, the same weight as a major bitter-acid signal, together with W4–W6 and W17, whose information is mostly noise; they also recovered same-cultivar pairs less well than Pareto scaling in I_abs and I_rel (median partner rank 4–5 against 3). Mean-centering alone went to the other extreme and let the largest signal dominate: humulone accounted for 66 % of the variance of I_abs, 29 % of I_rel and 70 % of Q_abs, so that the analysis became, in effect, an analysis of the humulone content.

Table A9. Comparison of pretreatments: variance explained by three principal components, the variable with the largest share of the variance, the share of the blank window W18, the median rank of the nearest same-cultivar sample (same product form) and of the pellet–Cryo partner, the silhouette width of the region of growth and of the solvent bottle (within S1), and the leave-one-cultivar-out balanced accuracy of a 3-nearest-neighbor classifier for the region of growth.

Pretreatment	PC1–3 (%)	Largest variable (% of variance)	Blank W18 (%)	Same-cultivar rank	Pellet–Cryo rank	Silhouette, region	Silhouette, bottle	k-NN region
I_abs — 21 windows, mmol/kg								
mean-centering	97.4	W09 (66)	0.0	5	38.5	0.02	-0.01	0.42
autoscaling	89.9	W02 (5)	4.8	5	40.5	-0.00	0.08	0.40
Pareto	94.5	W09 (32)	0.2	3	39.5	0.04	0.02	0.56
range	89.4	W18 (7)	6.6	4	40.0	-0.01	0.09	0.39
level	94.7	W18 (55)	54.6	11	39.5	-0.02	0.19	0.49
VAST	92.8	W13 (8)	0.2	4	38.0	0.01	0.07	0.34
glog + Pareto	87.7	W20 (9)	5.3	4	38.5	-0.01	0.05	0.44
I_rel — 21 windows per 100 major signals								
mean-centering	93.9	W09 (29)	0.0	2	3.5	0.00	0.01	0.44
autoscaling	77.7	W02 (5)	4.8	5	10.5	-0.04	0.04	0.53
Pareto	88.1	W09 (16)	0.5	3	5.5	-0.01	0.01	0.48
range	82.8	W11 (8)	2.5	4	7.0	-0.02	0.03	0.50
level	97.4	W18 (87)	87.0	11	32.5	-0.13	0.17	0.52
VAST	80.3	W09 (15)	0.0	3	4.0	-0.01	0.03	0.43
glog + Pareto	81.6	W20 (12)	7.0	4	8.5	-0.08	0.03	0.48
Q_abs — 8 components, % w/w								
mean-centering	98.8	humulone (70)	—	4	38.5	0.03	0.00	0.50
autoscaling	95.4	cohumulone (13)	—	3	39.0	0.03	0.04	0.46
Pareto	96.8	humulone (39)	—	2	38.0	0.04	0.02	0.48
range	95.6	cohumulone (18)	—	3	39.5	0.03	0.03	0.44
level	94.9	myrcene (eq.) (22)	—	5	40.0	0.02	0.03	0.51
VAST	96.2	adlupulone (21)	—	4	38.5	0.03	0.05	0.41

Pretreatment	PC1–3 (%)	Largest variable (% of variance)	Blank W18 (%)	Same-cultivar rank	Pellet–Cryo rank	Silhouette, region	Silhouette, bottle	k-NN region
glog + Pareto	94.6	α-humulene (21)	—	3	39.0	-0.02	0.00	0.37
clr + Pareto	93.0	α-humulene (19)	—	2	6.0	-0.05	-0.00	0.50
Q_rel — 8 components, % of sum								
mean-centering	96.7	humulone (37)	—	3	2.0	0.01	0.01	0.36
autoscaling	89.3	colupulone (13)	—	2	8.5	-0.02	0.00	0.49
Pareto	93.7	humulone (25)	—	2	3.0	-0.00	0.01	0.45
range	90.4	colupulone (15)	—	2	6.5	-0.02	0.01	0.53
level	90.4	α-humulene (19)	—	2	9.5	-0.03	0.00	0.43
VAST	90.9	humulone (22)	—	2	7.0	-0.02	0.00	0.47
glog + Pareto	92.0	α-humulene (24)	—	2	6.0	-0.05	-0.00	0.46
clr + Pareto	93.1	α-humulene (20)	—	2	5.5	-0.05	-0.00	0.48

All combinations (60) are given in the companion workbook. glog: generalized logarithm with λ equal to the noise variance of W18 (integral data) or of 0.02 % w/w (components); clr: centered log-ratio. Chance balanced accuracy 0.33.

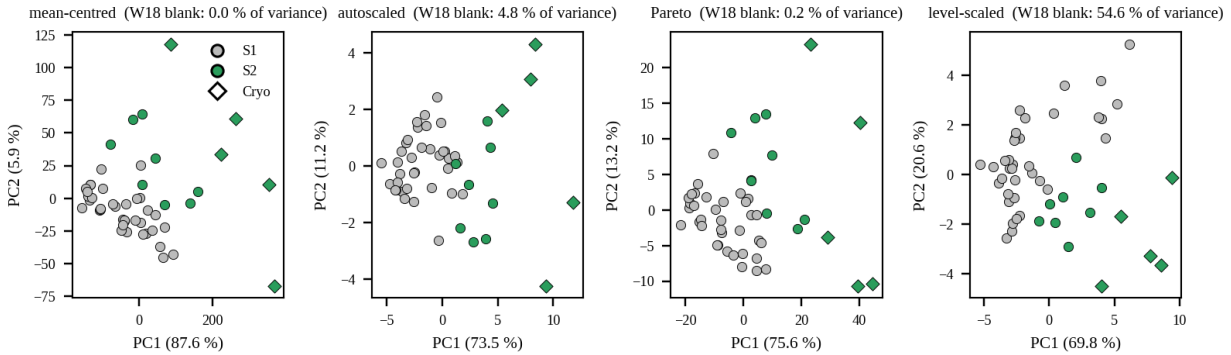

Figure A8. Scores on the first two principal components of the integral data set I_abs (mmol/kg) after four pretreatments, with the share of the total variance carried by the blank window W18. Gray: set S1; green: set S2; diamonds: Cryo pellets. The level-scaled map is dominated by the blank and separates the two measurement campaigns.

Pareto scaling kept the blank below 1 % of the variance in both integral data sets (0.2 % in I_abs, 0.5 % in I_rel) while limiting the largest variable to 32 % (I_abs) and 16 % (I_rel), and it gave the best or joint-best recovery of same-cultivar pairs in I_abs, Q_abs and Q_rel, the median rank of the nearest same-cultivar sample being 3 in the integral data sets and 2 in the component data sets; only in I_rel did mean-centering alone do slightly better (rank 2), at the price of the dominance of humulone. VAST scaling suppressed the blank as effectively, since the coefficient of variation of a noise variable is very large, but recovered same-cultivar pairs slightly less well in I_abs (rank 4) and gave the lowest nearest-neighbor accuracy for region (0.34). The generalized logarithm did not help: by compressing the large signals it raised the relative weight of the noise, and the blank share rose to 5–9 %. For the component data the centered log-ratio transformation performed as well as Pareto scaling of the closed composition, with a partner rank of 2 in both.

None of the pretreatments produced a geographic structure. The silhouette widths of the region of growth in the first three principal components lie between −0.13 and 0.04 for all sixty combinations, the nearest-neighbor balanced accuracy for region between 0.32 and 0.56, and the solvent-bottle silhouette within S1 between −0.03 and 0.20, the highest values belonging to level scaling. Mean-centering followed by Pareto scaling, the PNA default, is therefore supported by the data as well as by convention, and it was used for every analysis that follows; the choice between it and the centered log-ratio for compositional data is

immaterial here. The absolute data sets were not log-transformed, since the amount of extract, which the logarithm would compress, is itself one of the properties of interest.

A8. Unsupervised Analysis

A8.1 Principal Components of the Integral Data

The principal component analysis of the integrals on the absolute scale, I_abs, is shown in Figure A9 and summarized, with that of the other three data sets, in Table A10. The first component accounts for 75.6 % of the variance and is an axis of amount: its scores are correlated with the total α-acid content (r = 0.96), the myrcene-type diene (0.91), α-humulene (0.94) and the β-acids (0.74), and its loadings are positive for every window, with the largest weights on humulone, the myrcene diene, cohumulone and adhumulone. It separates the five Cryo pellets and the two fresh New Zealand high-α hops of 2023–2024 at its positive end from the old, low-α European landraces at its negative end, and its correlation with the Cryo form (0.76) and with membership of set S2 (0.72) shows that it combines three things that cannot be separated in these samples: the resin content of the cultivar, the lupulin enrichment of the product and the freshness of the lot. The second component (13.2 %) is the α/β balance (r = −0.68 with log α/β; 0.66 with the β-acid content), and the third (5.7 %) is the co-homolog fraction (r = 0.85 with the cohumulone and 0.86 with the colupulone fraction), mixed with the ratio of oil to resin (−0.61). Element-wise cross-validation gave Q^2 values of 0.62, 0.79 and 0.84 for one to three components and no improvement beyond three, whereas the broken-stick rule retained two components and parallel analysis one, a disagreement of the usual kind that is resolved here by the chemical interpretability of the third. Four of the Cryo pellets, Vic Secret and Enigma exceed the 95 % T^2 limit, as their extreme contents or cohumulone fractions require, and three Cryo pellets exceed the Q limit, which reflects the fixed-window bias in their α-acid homologs as much as any genuine peculiarity.

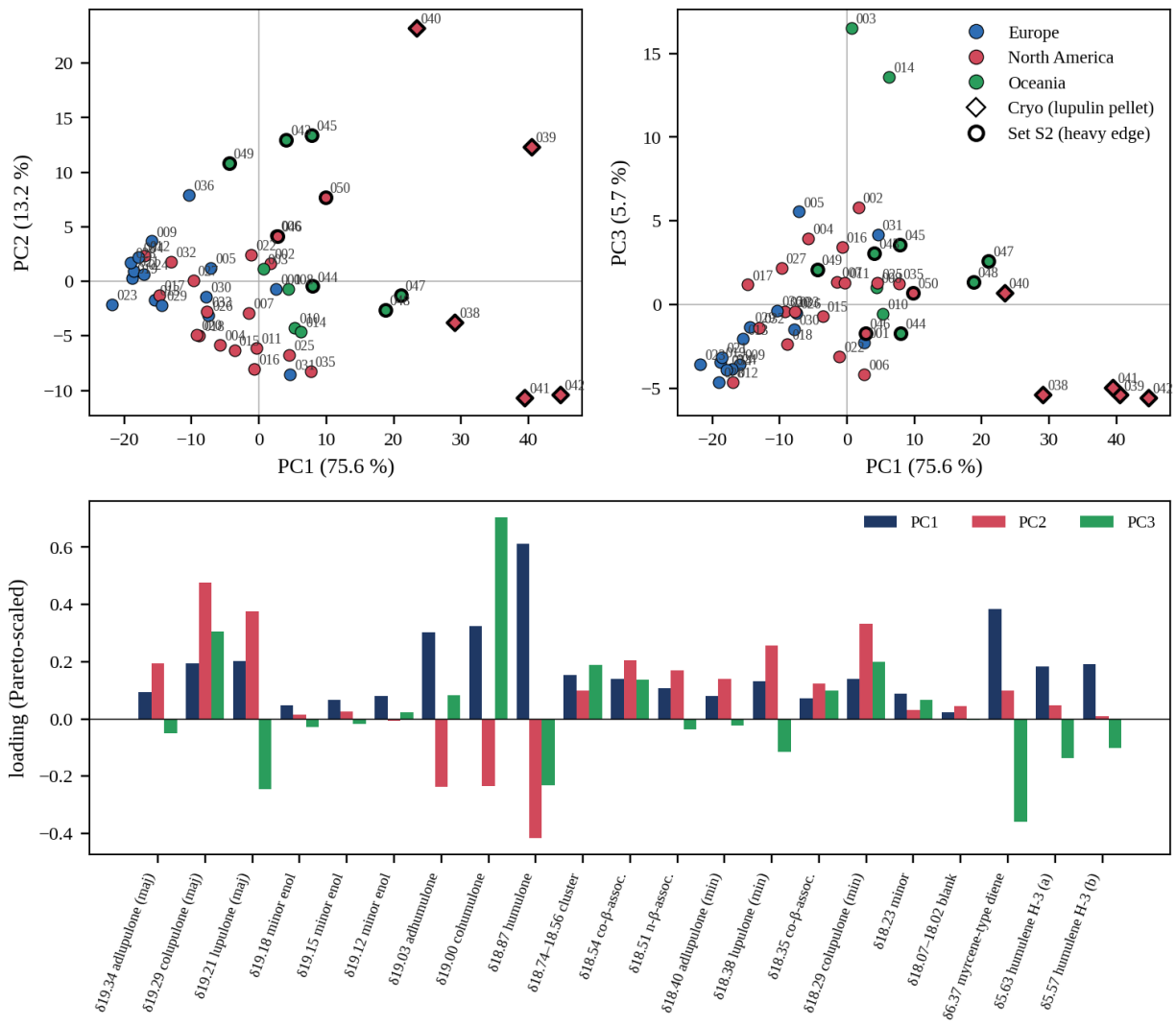

Figure A9. Principal component analysis of the integral data set on the absolute scale (I_abs, 21 windows in mmol/kg, mean-centered and Pareto-scaled): scores on PC1–PC2 and PC1–PC3, colored by region of growth (diamonds: Cryo pellets; heavy outlines: set S2), and loadings of the first three components.

In the compositional form, I_rel, the amount of extract cancels and the structure described in v1.1 reappears, now with the terpene windows added (Figure A10). The first component (60.8 %) is the α/β ratio, with a correlation of 0.99 with its logarithm; the second (18.6 %) opposes the co-homolog fraction ($r = -0.89$ with cohumulone, −0.79 with colupulone) to the ratio of oil to resin (0.79); and the third (8.7 %) is again an oil component, correlated with the myrcene diene and with membership of S2. Two chemical dimensions of the bitter acids, which v1.1 related to two distinct steps of their biosynthesis, therefore survive the change of scale and the enlargement of the data set, and a third, an oil dimension, is added by the terpene windows; it describes the freshness and the product form of the sample rather than its genotype. Vic Secret alone exceeds the T^2 limit, through its cohumulone fraction of 50 %, and the Saaz, the retail Amarillo and the Huell Melon exceed the Q limit.

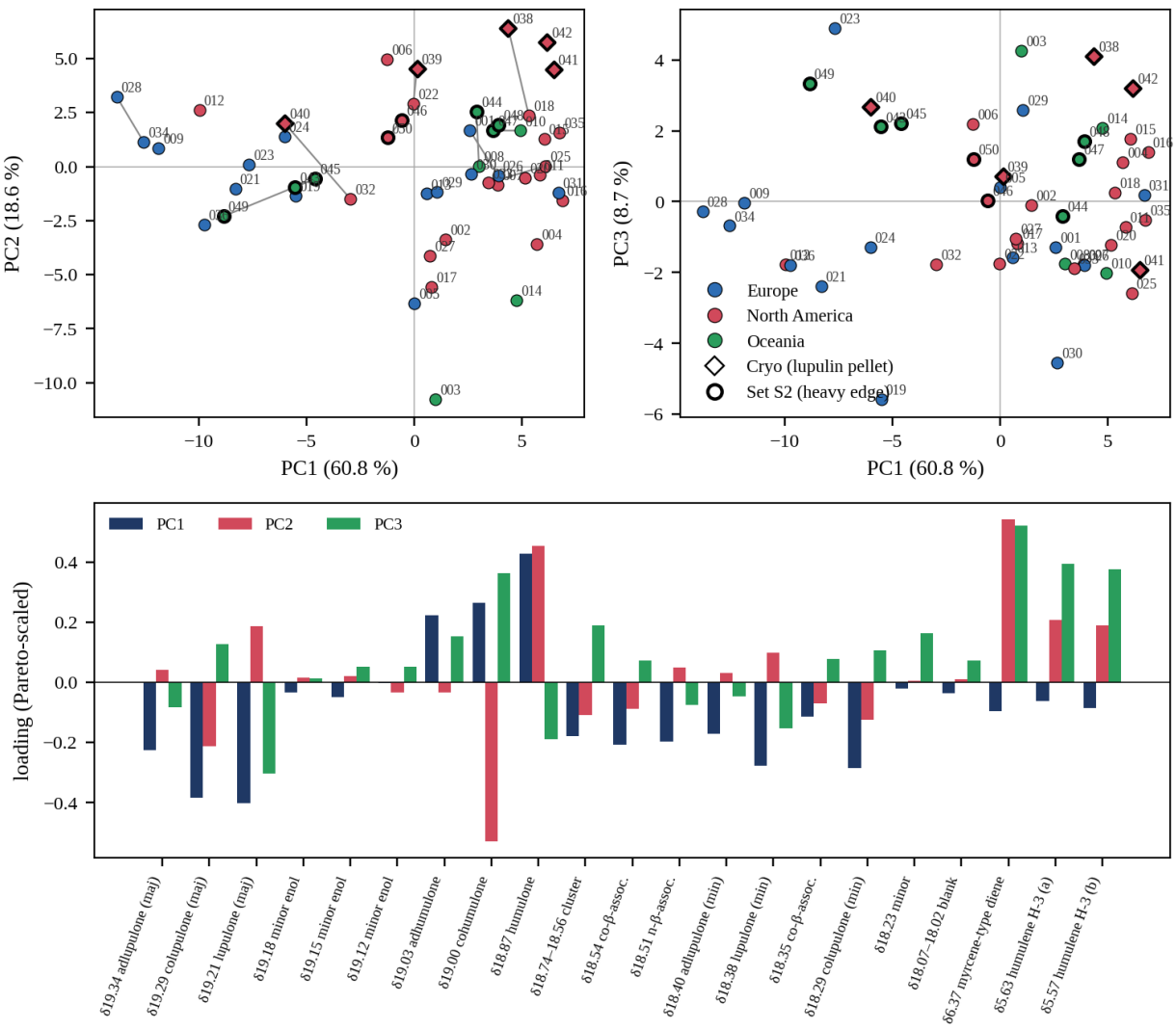

Figure A10. Principal component analysis of the integral data set in compositional form (I_rel, 21 windows per 100 units of the six major bitter-acid signals, mean-centered and Pareto-scaled). Gray lines join samples of the same cultivar. Symbols as in Figure A9.

The lines that join samples of the same cultivar in Figure A10 show what composition can and cannot do. The distance between two samples of the same cultivar in the space of the first three components is 0.12–0.78 of the median distance between all pairs, and for the Hersbrucker pair, the 2023 and 2024 Wakatu and the two HBC 1019 samples the partner is the nearest neighbor; the three Wakatu harvests form a tight group, and the Cryo and retail Amarillo lie close together. The Cryo and retail pellets of Centennial and Cascade are farther apart (0.69 and 0.78 of the median distance), partly because of the oil dimension and partly because of the window bias in the cohumulone fraction of the Cryo extracts. Same-cultivar samples are thus closer than random pairs, as they were in v1.1, but they are not reliably each other's nearest neighbors, and in the absolute data set the Cryo–pellet pairs are separated by more than twice the median distance.

A8.2 Principal Components of the Component Data

The component data sets reproduce the same structure with fewer variables (Figure A11). In Q_abs the first three components account for 75.2, 15.6 and 6.1 % of the variance and are again amount ($r = 0.97$ with the

α-acids), α/β balance and co-homolog fraction; in Q_rel they account for 70.0, 18.1 and 5.7 % and are the α/β ratio (r = 1.00 with its logarithm), the co-homolog fraction (0.97 with cohumulone) and the oil fraction (0.57 with the myrcene diene and 0.55 with membership of S2). The biplots show the expected geometry: the three α-acid homologs point toward the high-α samples, the three β-acid homologs toward the β-rich landraces, cohumulone and colupulone toward the high-cohumulone cultivars, and the two terpenes toward the Cryo pellets and fresh lots. Nothing in the component data is lost relative to the integral data except the weak independent signals of Section A3.4, which contribute little variance after Pareto scaling.

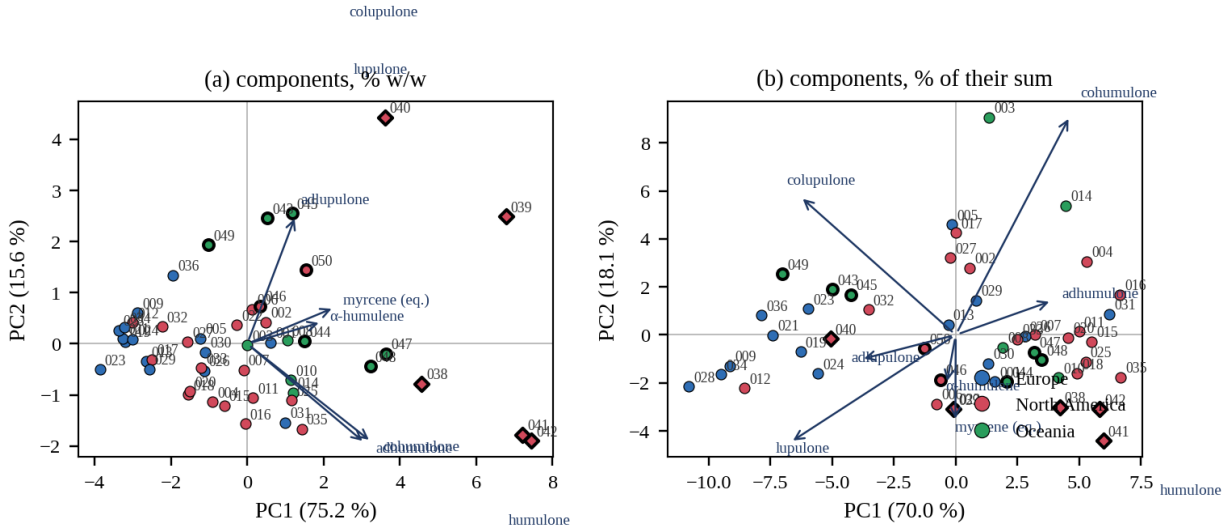

Figure A11. Principal component biplots of the component data sets: (a) the eight quantified constituents in % w/w (Q_abs); (b) the same as percentages of their sum (Q_rel). Mean-centered and Pareto-scaled; arrows are loadings scaled to the score range.

Table A10. Principal component analysis of the four data sets (mean-centered, Pareto-scaled): explained variance, cross-validated Q² (element-wise k-fold), number of components retained by the broken-stick rule and by parallel analysis, and interpretation from the correlation (r) of the scores with chemical descriptors.

Data set	Explained variance PC1 / PC2 / PC3 (%)	Q² for 1 / 2 / 3 PCs	Broken stick / parallel analysis	Interpretation (correlation r)
I_abs	75.6 / 13.2 / 5.7	0.62 / 0.78 / 0.84	2 / 1	PC1 amount (α 0.96, myrcene 0.91, Cryo 0.76, S2 0.72); PC2 α/β (log α/β −0.68); PC3 co-fraction (co-α 0.85, co-β 0.86), oil/resin −0.61
I_rel	60.8 / 18.6 / 8.7	0.51 / 0.64 / 0.60	2 / 2	PC1 α/β (log α/β 0.99); PC2 co-fraction (co-α −0.89, co-β −0.79) vs oil/resin (0.79); PC3 oil (myrcene 0.44, S2 0.43)
Q_abs	75.2 / 15.6 / 6.1	0.56 / 0.74 / 0.84	1 / 1	PC1 amount (α 0.97, humulene 0.93); PC2 α/β (β 0.69, log α/β −0.66); PC3 co-fraction (co-α 0.88, co-β 0.90)
Q_rel	70.0 / 18.1 / 5.7	0.55 / 0.76 / 0.77	1 / 1	PC1 α/β (log α/β 1.00); PC2 co-fraction (co-α 0.97, co-β 0.91); PC3 oil (myrcene 0.57, S2 0.55)

Oil/resin: logarithm of the ratio of the myrcene diene to the six major bitter-acid signals. S2 and Cryo: indicator variables for membership of set S2 and for the Cryo form.

A8.3 Hierarchical Clustering: Chemotypes and Content Classes

Ward clustering of the compositional integral data, I_rel, gave the partition shown in Figure A12a and described in Table A11. The silhouette width was greatest for two clusters (0.44), and the three-cluster solution, which is the more informative chemically, had cluster stabilities of 0.94, 0.61 and 0.84 (mean bootstrap Jaccard coefficients) and agreed closely with k-means (adjusted Rand index 0.94) and with complete linkage (0.88). The first cluster, of 14 samples, is the β-rich chemotype, with molar α/β ratios of

0.43–1.15: the German, Czech and Slovenian landraces and their derivatives (Saaz, Spalt, Hallertau, both Hersbrucker samples, Savinjski Golding, the unspecified German hop, Huell Melon), Crystal, the retail and Cryo Cascade, and all three Wakatu harvests. The second, of eight samples, is the high-cohumulone chemotype (median cohumulone 36 %, colupulone 60 %): Galena, Vic Secret, Idaho 7, Ariana, Enigma, Bravo, Northern Brewer and Cluster. The third, of 27 samples, is the α-rich chemotype (median α/β 2.7), which contains every other cultivar, including the Cryo Centennial, Amarillo, Simcoe and Mosaic, Nelson Sauvin, Waimea, Nectaron and HBC 1019. The three clusters correspond to the β-rich, high-cohumulone and α-rich clusters of v1.1. The β-rich cluster again contains ten S1 samples, the European landraces with Crystal and Cascade, now joined by the Cryo Cascade and the three Wakatu harvests; the high-cohumulone cluster shares six of its eight members with that of v1.1 (Galena, Cluster, Northern Brewer, Ariana, Vic Secret and Enigma), Idaho 7 and Bravo having joined it and Perle and the Traditional German having moved to the α-rich cluster in the present, larger variable set.

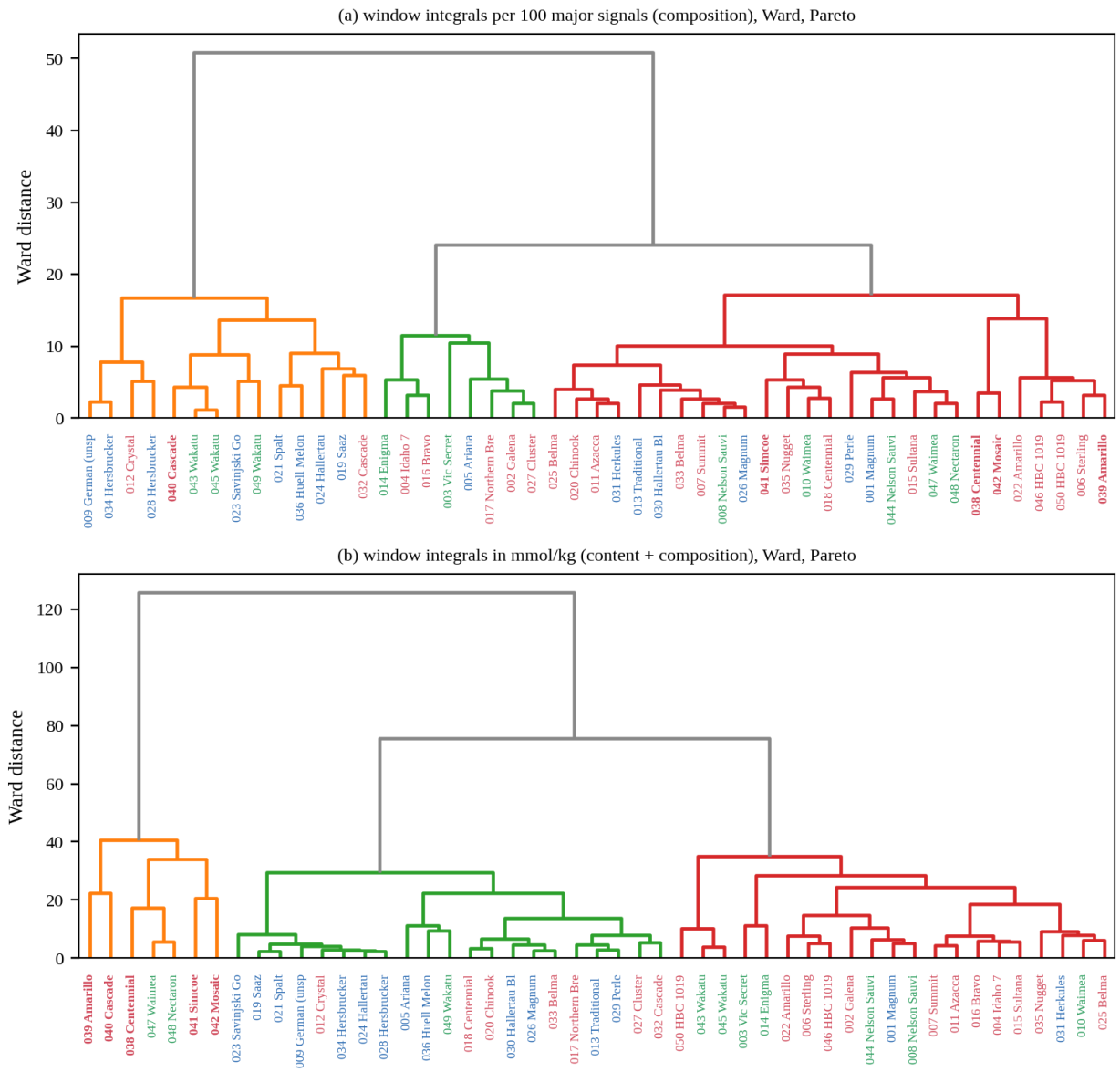

Figure A12. Ward dendrograms (Euclidean distance, mean-centered and Pareto-scaled data): (a) the compositional integral data set I_rel, in which the three clusters are the β-rich, high-cohumulone and α-rich chemotypes; (b) the integral data set on the absolute scale, I_abs. Leaf labels are colored by region of growth (blue Europe, red North America, green Oceania); Cryo pellets are in bold.

Table A11. The three-cluster Ward partitions of the compositional (I_rel) and absolute (I_abs) integral data sets: bootstrap stability (mean Jaccard coefficient), median composition and membership.

Cluster	Jaccard	α/β median (range)	co-α (%)	co-β (%)	α (%) / myrcene (%)	Members
Chemotypes (I_rel, Ward, k = 3)						
β-rich (n = 14)	0.94	0.78 (0.43–1.15)	26.2	46.4	1.9 / 0.22	009 German (unspecified), 012 Crystal, 019 Saaz, 021 Spalt, 023 Savinjski Golding, 024 Hallertau, 028 Hersbrucker, 032 Cascade, 034 Hersbrucker, 036 Huell Melon, 040 Cascade, 043 Wakatu, 045 Wakatu, 049 Wakatu
high-cohumulone (n = 8)	0.61	2.07 (1.71–4.98)	35.9	60.3	8.8 / 0.29	002 Galena, 003 Vic Secret, 004 Idaho 7, 005 Ariana, 014 Enigma, 016 Bravo, 017 Northern Brewer, 027 Cluster

Cluster	Jaccard	α/β median (range)	co-α (%)	co-β (%)	α (%) / myrcene (%)	Members
α-rich (n = 27)	0.84	2.66 (1.50–4.75)	24.5	47.8	10.3 / 0.59	001 Magnum, 006 Sterling, 007 Summit, 008 Nelson Sauvin, 010 Waimea, 011 Azacca, 013 Traditional German, 015 Sultana, 018 Centennial, 020 Chinook, 022 Amarillo, 025 Belma, 026 Magnum, 029 Perle, 030 Hallertau Blanc, 031 Herkules, 033 Belma, 035 Nugget, 038 Centennial, 039 Amarillo, 041 Simcoe, 042 Mosaic, 044 Nelson Sauvin, 046 HBC 1019, 047 Waimea, 048 Nectaron, 050 HBC 1019
Content classes (I_abs, Ward, k = 3)						
low content (n = 21)	0.79	1.15 (0.43–3.55)	26.9	48.3	3.6 / 0.24	005 Ariana, 009 German (unspecified), 012 Crystal, 013 Traditional German, 017 Northern Brewer, 018 Centennial, 019 Saaz, 020 Chinook, 021 Spalt, 023 Savinjski Golding, 024 Hallertau, 026 Magnum, 027 Cluster, 028 Hersbrucker, 029 Perle, 030 Hallertau Blanc, 032 Cascade, 033 Belma, 034 Hersbrucker, 036 Huell Melon, 049 Wakatu
medium content (n = 21)	0.78	2.32 (0.95–4.98)	27.4	49.6	9.9 / 0.59	001 Magnum, 002 Galena, 003 Vic Secret, 004 Idaho 7, 006 Sterling, 007 Summit, 008 Nelson Sauvin, 010 Waimea, 011 Azacca, 014 Enigma, 015 Sultana, 016 Bravo, 022 Amarillo, 025 Belma, 031 Herkules, 035 Nugget, 043 Wakatu, 044 Nelson Sauvin, 045 Wakatu, 046 HBC 1019, 050 HBC 1019
high content (n = 7)	0.85	2.93 (0.94–4.44)	22.1	47.1	18.3 / 1.81	038 Centennial, 039 Amarillo, 040 Cascade, 041 Simcoe, 042 Mosaic, 047 Waimea, 048 Nectaron

Adjusted Rand index of the chemotypes with the region of growth 0.07, with the region of breeding 0.07, with k-means 0.94 and complete linkage 0.88. Content classes: adjusted Rand index with product form 0.21 and with measurement set 0.24 (0.77 and 0.51 for k = 2).

The placement of Wakatu with the European landraces is the most instructive result of the clustering. Wakatu was bred in New Zealand and released in 1988 as "New Zealand Hallertau Aroma", a triploid whose parentage is two-thirds Hallertau Mittelfrüh,[52] and its bitter-acid composition is that of its European parent, not that of the other New Zealand cultivars, Nelson Sauvin, Waimea and Nectaron, which fall in the α-rich cluster. The chemotype follows the genotype and not the country in which the hop was grown or bred. The adjusted Rand index between the three chemotypes and the region of growth is 0.07, and that with the region of breeding also 0.07.

Clustering of the absolute data, I_abs, produces classes of content rather than of composition (Figure A12b). The two-cluster solution (silhouette 0.55) separates the Cryo pellets and the fresh high-α New Zealand hops of 2023–2024 from everything else and agrees with the product form (adjusted Rand index 0.77) and with the measurement set (0.51) far better than with the region of growth (−0.01). The three-cluster solution divides the remainder into low-content samples (median α-acids 3.6 %), which are the landraces, the low-α American aroma cultivars and several old S1 lots, and medium-content samples (median 9.9 %). These clusters are real in the sense that they are stable (Jaccard 0.78–0.85) and describe the samples correctly, but they classify the hops by how much resin and oil they contain as purchased, which is a property of the product and its history as much as of the cultivar.

A8.4 UMAP and t-SNE

The two-dimensional UMAP and *t*-SNE maps of the four data sets are shown in Figures A13 and A14, and three-dimensional versions of both, together with the principal component scores, are provided in the interactive viewer that accompanies this addendum. The maps reproduce the groupings found by PCA and HCA, the Cryo pellets and fresh high-α lots in the absolute data and the β-rich chemotype in the compositional data, and they show them more dramatically: in the UMAP map of Q_rel, for example, the β-rich chemotype becomes a separate island, although in the principal component map it is the end of a continuum of α/β ratios.

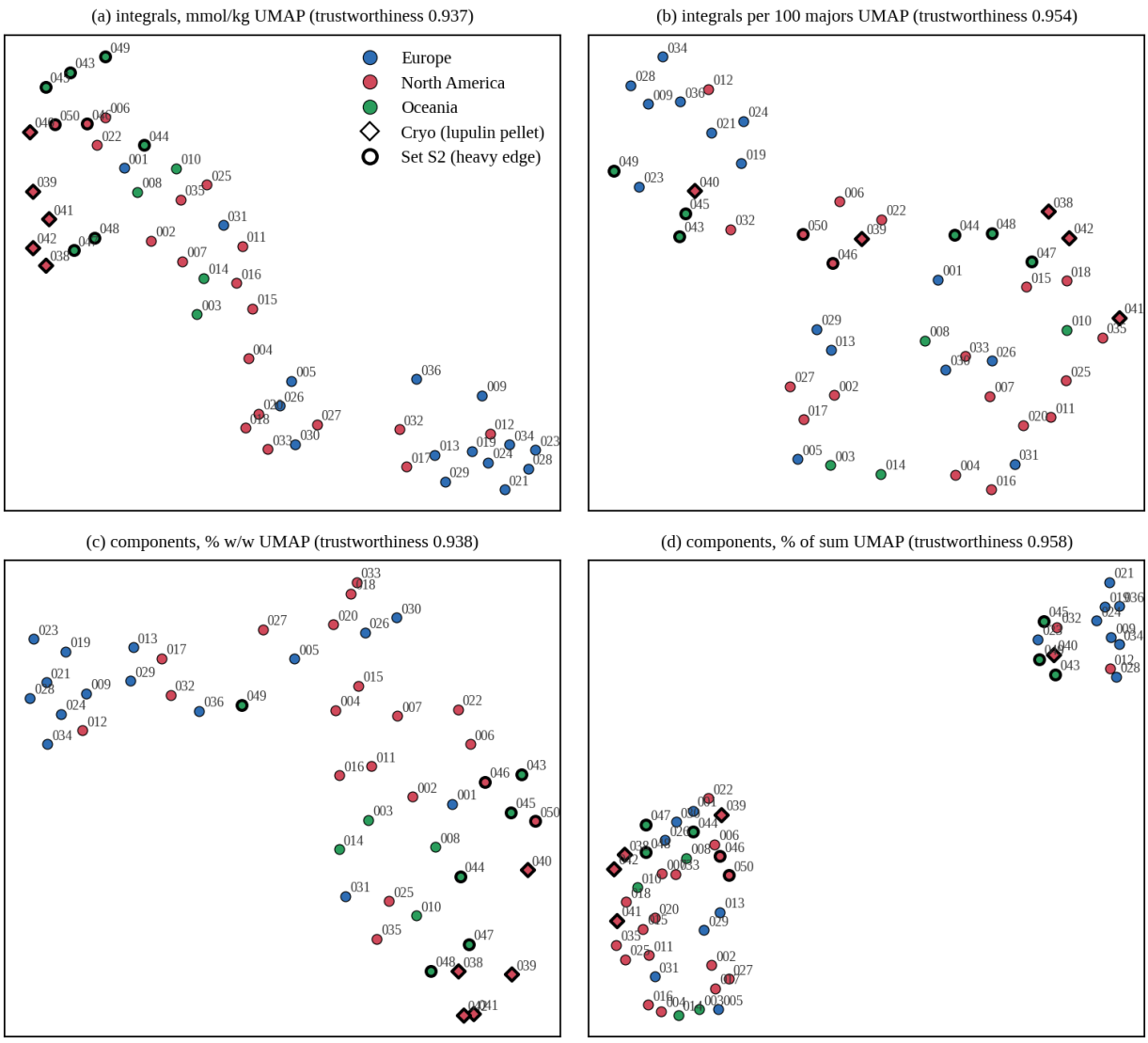

Figure A13. Two-dimensional UMAP embeddings (8 neighbors, minimum distance 0.3) of the four data sets, with trustworthiness. Symbols as in Figure A9. Distances between groups in these maps have no quantitative meaning.

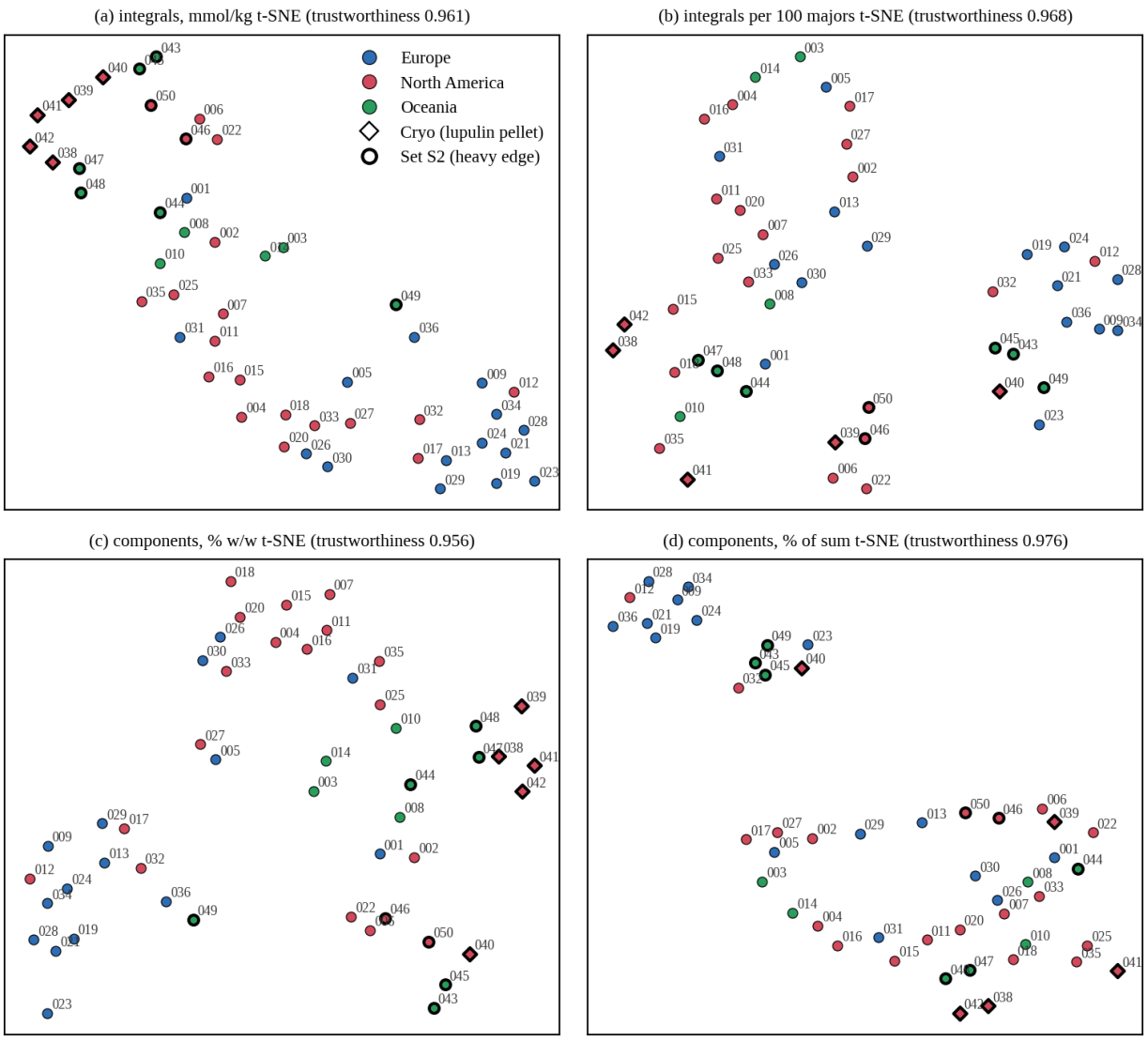

Figure A14. Two-dimensional *t*-SNE embeddings (perplexity 8, principal-component initialization) of the four data sets, with trustworthiness. Symbols as in Figure A9.

The drama is not a gain in information, and Table A12 shows why. All the two-dimensional maps have high trustworthiness (0.94–0.98), a measure that rewards the absence of false neighbors, but when the five nearest neighbors of each sample in the full pretreated data are compared with its five nearest neighbors in the map, the three-component PCA retains 84–91 % of them, whereas UMAP retains 71–74 % and *t*-SNE 74–79 %. The neighborhoods found by UMAP also changed with the random seed (82–83 % agreement between seeds); those of *t*-SNE did not, because the principal-component initialization makes it deterministic. With data whose effective dimension is three, the principal component map is the more faithful representation, and the nonlinear embeddings are best used, as experienced users and critics of these methods both advise,[40,41] to look for local structure that is then confirmed in the original data, and not to judge the size of gaps between groups.

Table A12. Faithfulness of the low-dimensional maps: trustworthiness (5 neighbors), fraction of each sample's five nearest neighbors in the full pretreated data retained in the two-dimensional map (three-dimensional for PCA), and agreement of UMAP neighborhoods between ten random seeds.

Data set	PCA 2D	PCA 3D	UMAP 2D	UMAP 3D	t-SNE 2D	t-SNE 3D	5-NN kept, PCA 3D	5-NN kept, UMAP	5-NN kept, t-SNE	UMAP seed agreement
I_abs	0.955	0.994	0.937	0.944	0.961	0.967	0.87	0.71	0.77	0.82
I_rel	0.956	0.988	0.954	0.965	0.968	0.900	0.84	0.72	0.76	0.82
Q_abs	0.960	0.997	0.938	0.960	0.956	0.941	0.91	0.71	0.74	0.83
Q_rel	0.967	0.994	0.958	0.975	0.976	0.968	0.88	0.74	0.79	0.83

t-SNE with principal-component initialization is deterministic (seed agreement 1.00).

A8.5 Geography in the Unsupervised Maps

In none of the maps does the region of growth or the region of breeding organize the samples. The silhouette widths of the region of growth lie between −0.01 and 0.04 in the Pareto-scaled data sets, the adjusted Rand indices between the clusters and the regions do not exceed 0.18 for any number of clusters from two to five, and in every score plot European, North American and Oceanian samples are interleaved. Where samples of one region do group together, as the German landraces do, the grouping is shared with cultivars of the same lineage grown elsewhere, as the case of Wakatu shows, and it is the lineage, not the region, that the data follow.

A9. Supervised Classification

A9.1 The Positive Control: Product Form

The ability of the procedure to find a difference that is known to exist was tested first. The Cryo pellets contain about twice the lupulin of conventional pellets, and a classifier given the absolute data should recognize them. It did: under leave-one-cultivar-out validation, logistic regression and SIMCA on I_abs and SIMCA on Q_abs reached a balanced accuracy of 0.99, and the radial-basis SVM on Q_abs 0.98 (Table A13). On the compositional data sets, from which the amount of extract cancels, the best results were lower, 0.79 (I_rel) and 0.82 (Q_rel), and PLS-DA on Q_rel was at chance (0.50). The validation scheme is therefore capable of detecting a real difference. The control is nevertheless a modest one. A classifier given only the declared α-acid content reached 0.81, because four of the five Cryo products are declared at 16.1–25.6 % α-acids, a range reached by only three of the 44 pellets, and one given only the logarithm of the α/β ratio and the cohumulone and colupulone fractions reached 0.78, because four of the five Cryo products have measured cohumulone fractions of 17–22 %, below those of all but five pellets, a consequence partly of the cultivars chosen and partly of the window bias of Section A3.2. The results on the compositional data may therefore reflect the choice of cultivars as much as the higher ratio of oil to resin in the Cryo products. The task is made easier still by a confound, since all five Cryo pellets belong to the fresh set S2, and five positive samples are too few for a meaningful estimate of the sensitivity of a Cryo model.

A9.2 Region of Growth and Region of Breeding

The classification of the samples by the region in which they were grown and by the region in which the cultivar was bred is summarized in Table A13 and Figure A15. With three classes the chance level of the balanced accuracy is 0.33. The eight classifiers reached 0.34–0.59 for the region of growth and 0.38–0.61 for the region of breeding across the four data sets. PLS-DA, the method most often used for this purpose in food authentication, gave 0.45–0.48 for the region of growth and 0.38–0.47 for the region of breeding,

and the radial-basis SVM 0.41–0.49 and 0.38–0.47. The best single results were obtained by shrinkage LDA on I_abs for the region of growth (0.59) and by SIMCA on I_rel for the region of breeding (0.61).

The permutation tests put these figures in perspective. For PLS-DA the balanced accuracies exceeded the 95th percentile of the permutation distribution (0.42–0.48) only for the absolute data sets, with $p = 0.03$–0.05 for I_abs and Q_abs and $p = 0.07$–0.19 for the compositional data sets; for the radial-basis SVM the p-values were 0.08–0.25. When the selection of the best of five models was built into the permutation, as it must be if the best result is to be quoted, the best balanced accuracy for the region of growth on I_abs, 0.59, stood against a null distribution whose mean was 0.38 and whose 95th percentile was 0.53 ($p = 0.04$). For the region of breeding on I_abs the best result, 0.60, was reached by none of the 50 permutations (null mean 0.38, 95th percentile 0.52, $p = 0.02$, the smallest value attainable with 50 permutations), and on I_rel the best results, 0.59 for the region of growth and 0.61 for the region of breeding, stood against null means of 0.36 and 0.37 and 95th percentiles of 0.46 and 0.50 ($p = 0.04$ in both cases). A weak association between the NMR data and geography is therefore detectable, for PLS-DA only on the absolute data and for the best of several models on the compositional data as well; with p-values of 0.02–0.05 near the resolution of the tests and sixteen tests in all, the evidence is weak.

The baselines show what that association consists of. A classifier given nothing but the declared α-acid content, which requires no NMR measurement at all, reached 0.49 for the region of growth and 0.50 for the region of breeding, and one given only three chemical descriptors, the logarithm of the α/β ratio and the cohumulone and colupulone fractions, reached 0.56 and 0.61. No multivariate model exceeds the better of these two baselines by more than a few hundredths, and the three-descriptor baseline is itself compositional, which is consistent with the finding that the best compositional models are as good as the best absolute ones. What geographic information the data carry is the information carried by the breeding objectives of different regions, high α-acids in the American and Oceanian cultivars and low α-acids with high β-acids in the European landraces, and by the history of the samples, which is itself confounded with region in this data set: six of the ten Oceania samples and all five Cryo pellets belong to the fresh set S2.

Table A13. Balanced accuracy of classification by eight methods under leave-one-cultivar-out cross-validation with nested tuning (38 folds), with permutation p-values where computed, the best of five models with a selection-aware permutation test, and baseline classifiers.

Target / data set	PLS-DA	SVM lin.	SVM RBF	LDA	k-NN	Logist.	RF	SIMCA	Best of 5 (p)
Region of growth									
I_abs	0.45 (p 0.05)	0.54	0.48 (p 0.09)	0.59	0.56	0.44	0.38	0.51	0.59 (p 0.04)
I_rel	0.46 (p 0.07)	0.40	0.41 (p 0.22)	0.45	0.45	0.47	0.51	0.59	0.59 (p 0.04)
Q_abs	0.48 (p 0.03)	0.56	0.49	0.48	0.47	0.53	0.44	0.51	—
Q_rel	0.46 (p 0.09)	0.37	0.42	0.45	0.34	0.44	0.40	0.52	—
baselines	majority 0.33	declared α only 0.49	log α/β, co-α, co-β only 0.56						
Region of breeding									
I_abs	0.47 (p 0.03)	0.60	0.47 (p 0.08)	0.54	0.56	0.60	0.46	0.50	0.60 (p 0.02)
I_rel	0.42 (p 0.13)	0.45	0.40 (p 0.25)	0.41	0.40	0.47	0.49	0.61	0.61 (p 0.04)
Q_abs	0.47 (p 0.05)	0.51	0.47	0.47	0.49	0.54	0.49	0.50	—
Q_rel	0.38 (p 0.19)	0.39	0.38	0.38	0.43	0.39	0.38	0.52	—
baselines	majority 0.33	declared α only 0.50	log α/β, co-α, co-β only 0.61						
Product form (Cryo vs pellet)									
I_abs	0.80	0.80	0.87	0.90	0.80	0.99	0.80	0.99	—
I_rel	0.70	0.75	0.67	0.70	0.49	0.77	0.60	0.79	—
Q_abs	0.70	0.88	0.98	0.80	0.80	0.88	0.80	0.99	—
Q_rel	0.50	0.82	0.69	0.69	0.49	0.78	0.59	0.69	—

Target / data set	PLS-DA	SVM lin.	SVM RBF	LDA	k-NN	Logist.	RF	SIMCA	Best of 5 (p)
baselines	majority 0.50	declared α only 0.81	log α/β, co-α, co-β only 0.78						
Trade class (aroma / dual / bittering)									
I_abs	0.55	0.52	0.57	0.52	0.44	0.49	0.52	0.60	—
I_rel	0.62	0.35	0.51	0.55	0.57	0.52	0.62	0.57	—
Q_abs	0.55	0.42	0.57	0.57	0.52	0.55	0.55	0.57	—
Q_rel	0.62	0.55	0.55	0.59	0.54	0.55	0.60	0.63	—
baselines	majority 0.33	declared α only 0.49	log α/β, co-α, co-β only 0.64						

Chance: 0.33 (three classes), 0.50 (product form). Permutation of labels among cultivars with the full nested procedure repeated: 100 permutations (PLS-DA), 50 (SVM RBF; 100 for I_abs, region of growth), 50 (best of PLS-DA, LDA, k-NN, logistic regression and SIMCA); p = (1 + number of permuted results ≥ observed)/(1 + number of permutations), so that the smallest attainable p is 0.01 with 100 and 0.02 with 50 permutations. Baselines use the same validation; the best of logistic regression, RBF-SVM and LDA is shown.

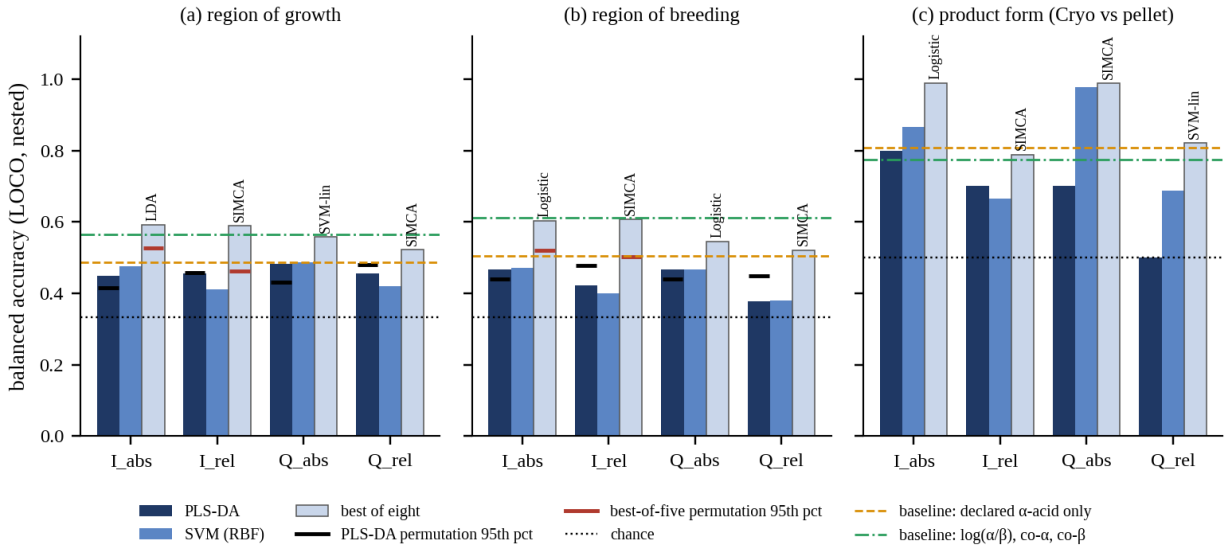

Figure A15. Balanced accuracy of leave-one-cultivar-out classification (nested tuning) for the region of growth (a), the region of breeding (b) and the product form (c). Bars: PLS-DA, radial-basis SVM and the best of eight classifiers for each data set (the best model is named above its bar); black ticks: 95th percentile of the PLS-DA permutation distribution; red ticks: 95th percentile of the selection-aware (best-of-five) permutation distribution, computed for I_abs and I_rel; dotted line: chance; dashed and dash-dotted lines: baseline classifiers (best of three models) using only the declared α-acid content and only the logarithm of the α/β ratio and the cohumulone and colupulone fractions.

A9.3 Confounding

Two checks were made to establish whether the weak geographic signal, and that of the absolute data in particular, is geographic at all. First, the measurement set proved to be highly predictable among the pellets: PLS-DA, LDA and SVM separated S1 from S2 with balanced accuracies of 0.81–0.94 on the absolute data sets, against 0.47–0.66 on the compositional ones. The absolute data thus encode the campaign, that is, the freshness of the lots and the product mix, far more strongly than they encode geography. The solvent bottle within S1 was weakly predictable from the absolute data (0.60–0.66 for PLS-DA and LDA) and not from the compositional data (0.40–0.60), which is consistent either with a small difference between the two calibrations or with the chance distribution of cultivars between the bottles, and the two cannot be distinguished. Second, the geographic classifications were repeated within S1 alone and within the pellets alone, removing the Cryo products and, in the first case, the campaign effect. The balanced accuracies then ranged from 0.27 to 0.67 with no consistent pattern, PLS-DA giving 0.37–0.52. The highest values in the

subsets, 0.60–0.67, obtained chiefly by LDA and the SVM on Q_abs and by LDA on I_abs, exceed those of the same models on the full data set, but with 36–44 samples, three classes and no permutation test they lie within the scatter seen between models, and they are not matched by comparable gains for the compositional data or for PLS-DA, the largest of which, from 0.46 to 0.52 for PLS-DA on I_rel within S1, is of the size of that scatter; they do not amount to evidence of a geographic signal hidden by the confounds.

A9.4 What the Classifiers Use

The PLS-DA display models of Figure A16, which are fitted to all 49 samples and are not validated, show the variables on which the region models rely. In both integral data sets the variables with importance in projection greater than one are the large signals, humulone, cohumulone, the major colupulone signal, the minor colupulone signal, the myrcene diene and, in I_rel, the major lupulone signal or, in I_abs, adhumulone, which is to say the amount and the α/β balance of the bitter acids and the oil content. None of the independent chelated enols of Section A3.4, which might have been expected to carry a regional marker if any existed, has an importance above 0.75. Even fitted to all the samples, the score plots show the three regions interleaved.

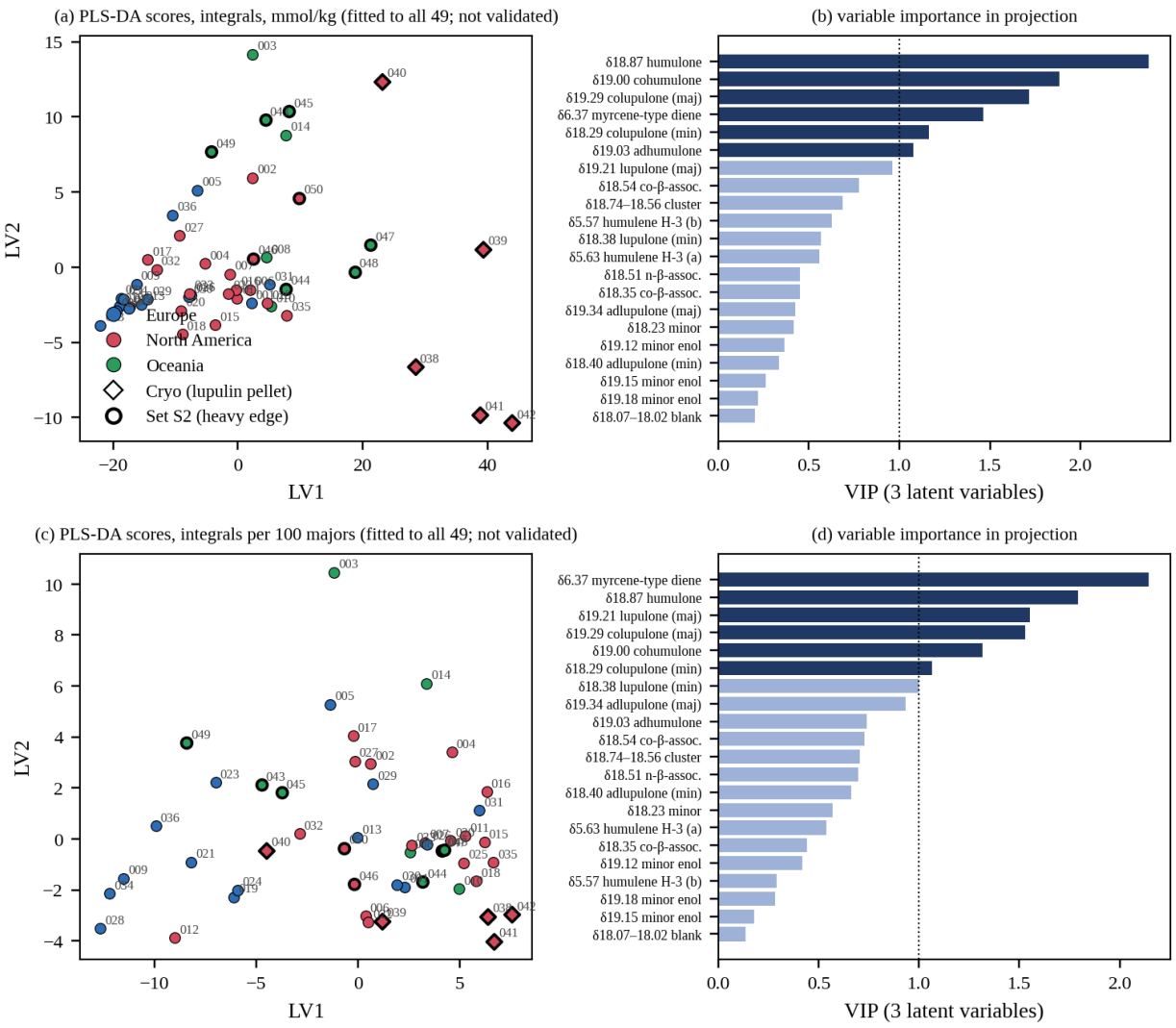

Figure A16. PLS-DA display models for the region of growth (three latent variables, fitted to all 49 samples; descriptive only): scores and variable importance in projection (VIP) for the integral data set on the absolute scale (a, b) and in compositional form (c, d). Dark bars: VIP > 1.

A9.5 The Trade Classification

The classification of the cultivars as aroma, dual-purpose or bittering hops reached balanced accuracies of 0.57–0.63 with the best model for each data set, against 0.64 for shrinkage LDA given only the logarithm of the α/β ratio and the cohumulone fraction. The trade classes are, in chemical terms, statements about the α/β ratio and, to a lesser extent, the cohumulone fraction, and the NMR data add nothing to those two numbers.

A9.6 Interpretation

The supervised results agree with the unsupervised ones and with v1.1. The ^{1}H NMR integrals of the hydroxyl region and of the two principal terpenes measure the genotype of a hop through its α/β ratio and co-homolog fractions, and the product and its history through the amounts of resin and oil; they do not carry a geographic signature that can be separated from those two sources of variation. That is what the published evidence on the geographic origin of hops would lead one to expect. In the ^{1}H NMR metabolite profiling

of thirteen commercial cultivars by Farag and co-workers, the separation of the cultivars was governed mainly by the ratio of α- to β-acids, and no separation by geographic region was observed, the Austrian and Czech lines clustering with German cultivars.[9] The methods that have discriminated the origin of hops rely instead on the stable isotope ratios of nitrogen and sulfur,[53] on major and trace elements, in a comparison of one cultivar grown at two sites,[54] or on volatile constituents measured by gas chromatography–mass spectrometry in the same cultivars grown in two countries.[55] The same aroma cultivars grown in the USA, Australia and Europe have also been compared directly,[56] and single-hop beers brewed with one cultivar grown in different regions have been shown to differ in their biochemical and sensory properties, to an extent that depended on the cultivar.[57] The oil dimension of the present data is too strongly dominated by storage losses to serve that purpose, and the two terpene windows measure only the two largest hydrocarbons.

The authentication problem that geography represents is, moreover, not the problem that a discriminant model solves. A discriminant model assigns every sample to one of the classes it was trained on; an authentication requires a model of the authentic class alone, with limits beyond which a sample is rejected, built from authenticated material and tested on samples it has not seen.[58,59] The present data set, with 49 samples of 38 cultivars and at most three lots of any one, can support neither. What it can support is the use of the homolog fractions and the α/β ratio as a consistency test against a declared cultivar, with a tolerance established from same-cultivar replicates, of which the three Wakatu harvests (cohumulone and colupulone fractions within 1.6 points) and the two HBC 1019 harvests (within 5.4 points) give the first estimates.

A10. What the Addendum Changes in Version 1.1

The addendum was written to be incorporated into PNA-WP-2026-HOPS-01, and the status of the statements of v1.1 that the new data bear upon is collected in Table A14. Most of the statistical inferences that v1.1 drew from the integral list without sight of the spectra have been confirmed, and the correspondence between the eighteen survey integrals of v1.1, which were listed in order of increasing chemical shift, and the windows of this addendum can now be stated: the survey integrals I3 to I8 of v1.1, which were identified there as the minor tautomer of colupulone (I3), a colupulone-associated signal at 0.10 of the major (I4), the minor tautomers of lupulone (I5) and adlupulone (I6), a β-associated signal of undetermined parent (I7) and a colupulone-associated signal at 0.25–0.34 of the major (I8), correspond to W16, W15, W14, W13, W12 and W11 respectively, and each identification is confirmed. The one parent that v1.1 could not identify, that of the signal now designated W12, is lupulone.

Table A14. Status of statements of PNA-WP-2026-HOPS-01 version 1.1 in the light of this addendum.

Statement in v1.1	Status	Evidence in this addendum
Survey integrals listed in order of shift; I10–I12 humulone, cohumulone, adhumulone; I16–I18 lupulone, colupulone, adlupulone (inferred)	Confirmed	Exact windows recovered from the spectra; peak positions within ±0.005 ppm (Table A2).
I6 = minor tautomer of adlupulone, δ 18.41 (probable, not proven)	Confirmed	Separately resolved line at δ 18.403; NNLS coefficient 0.44 on adlupulone (W13).
Tautomer ratio the same for the three β-acids (v1.0 claim of a colupulone-specific ratio withdrawn)	Confirmed	NNLS coefficients 0.44, 0.41 (+0.04), 0.46 (+0.06); overall minor/major 0.494 (SD 0.046).
I7 β-associated (parent undetermined); I8 colupulone-associated; the δ 18.55–18.48 window not an oxidation product	Refined	W11 (δ 18.537) ↔ colupulone 0.24; W12 (δ 18.511) ↔ lupulone 0.21; same ratio in old and fresh samples and in ICE-4.
ICE-4 test: α/β(major) ≈ 2.8 (minor tautomers only) or ≈ 3.4 (δ 18.5 pair too)	Performed	Observed 2.60; α/β with minor tautomers 1.705 vs 1.823 certified (−6.5 %); with the δ 18.5 pair 1.423 (−22 %). Counting rule: major + minor.
Total β uncertain by ~19 % pending assignment of the δ 18.5 pair	Resolved	δ 18.5 pair excluded from β; residual α/β bias −6.5 % (ICE-4).

Statement in v1.1	Status	Evidence in this addendum
co-β = 1.33 co-α + 11.6 (r^2 0.90, 36 samples)	Reproduced	S1: 1.327, 11.56, 0.897; all 49: 1.23, 15.4, 0.84 (Cryo window bias; Wakatu above the line).
PCA of the table normalized to adlupulone generates a spurious PC1 (divisor artifact)	Avoided	Absolute (mmol/kg) and per-100-majors data sets; no common divisor.
Two chemical dimensions: α/β ratio and co-homolog fraction	Confirmed; extended	I_rel PC1 60.8 % (α/β), PC2 18.6 % (co-fraction/oil); on the absolute scale an amount dimension (75.6 %) dominates; an oil dimension is added.
Three clusters: β-rich, high-cohumulone, α-rich	Confirmed	Same three chemotypes (Jaccard 0.94/0.61/0.84); Wakatu joins the European landraces.
No model of relative integrals replaces an internal standard (declared α not predictable; external failure)	Superseded for this data set	α-acids measured directly: S2 vs declared r = 0.975, RMS 1.84 %; absolute scale provisional (±10 %).
Region of breeding not classifiable beyond the label value	Confirmed	Best 0.61 vs 0.61 (three descriptors) and 0.50 (declared α only); geography not separable from genotype and product history.
Sample 026 “Magnum 8.9 %” possibly mislabeled	Supported	Composition matches Belma 033 (co-α 27.0/26.2, co-β 49.8/49.4, α/β 2.52/2.41), not Magnum 001.
Belma 025/033: replicate preparations or separate lots?	Not replicates	Different α/β (3.56/2.41) and α-acids (12.75/6.77 %) despite identical label and recorded mass.
Recommended protocol (Section 7.7): DMS internal standard in the extraction solvent, 25 s delay, ICE-4 control	Reaffirmed; amended	Add bracketing calibration if TMS transfer is kept, identical TMS windows, spectrum-specific α-acid windows or line fitting, dilution of concentrated extracts, recorded masses and bottles.

I-numbers refer to the eighteen survey integrals of v1.1 in order of increasing chemical shift.

Three changes are of substance. First, the question of how the upfield signals should be counted in the β-acid total, which v1.1 left open at about 19 %, has been settled by the ICE-4 measurement in favor of the minor tautomers alone, with a residual α/β bias of −6.5 % that should be quoted with any α/β ratio from the hydroxyl region. Second, the conclusion of v1.1 that no chemometric model of relative integrals can stand in place of an internal standard, which was demonstrated there by the failure of every model to predict the declared α-acid content of external samples, is superseded for this data set by the direct measurement: the α-acid contents are now obtained from the calibration and not from a model. The lesson of v1.1 remains valid for data without an absolute scale, and the direct measurement brings a difficulty of its own, the stability of the transfer standard, which v1.1 did not have to consider. Third, the recommended protocol of v1.1 (its Section 7.7) is reaffirmed and should be amended in four respects: the calibrant should be added to every tube, or, if the TMS transfer is retained, each bottle should be calibrated at the beginning and end of each batch; the TMS window should be identical in calibration and sample spectra; the α-acid windows should be set from each spectrum, or the α-acid triplet fitted, and concentrated extracts diluted to the pellet range; and the mass, bottle and date of every calibration and of every ICE-4 control should be recorded. It is suggested that the addendum be inserted into the main paper as a new section following its Section 9, with Sections 7.4, 7.7, 9.5 and 13.4 and the Summary revised to cross-refer to it.

A11. Critical Assessment and Recommendations

A11.1 What a Reviewer or an Opposing Expert Would Raise

The objections that an expert reviewer, an accreditation assessor or an opposing expert witness would be most likely to raise against the quantitative results of this addendum are, in order of weight, the following. The absolute scale rests on a volatile transfer standard whose content is known to have fallen in one of the two bottles and whose stability between the calibration and the extractions was not monitored; the one independent check of the scale, the ICE-4 extract, failed by almost a factor of two, and the explanation offered for the failure, a transcription of the mass, is plausible but unproven. Each sample was extracted and measured once, so that the repeatability of the method, and with it the significance of any difference between two samples, is unknown; the same-cultivar pairs are lots of different age and provenance and are

not replicates. The acquisition parameters other than the relaxation delay were not recorded, and the relaxation conditions of the calibration and sample spectra can be shown to be equivalent only by assumption. The declared α-acid contents with which the results were compared are nominal figures of unknown method and date, and agreement with them, although reassuring for the thirteen recent samples, is not validation. Two samples, the Belma 025 and the Magnum 026, carry labels or masses that are inconsistent with their spectra.

The assignment of the hydroxyl region is on firmer ground than in v1.1, because it now rests on resolved lines and exact windows as well as on statistics, but two points remain open: the identity of the δ 18.5 pair, which is fixed in proportion to the β-acid homologs but is apparently not measured as β-acid by the ICE-4 chromatographic assignment, and the fixed-window bias in the adhumulone–cohumulone split of concentrated extracts, which affects the cohumulone values of the Cryo pellets by several points.

For the chemometric results the principal objections are the size and structure of the data set, 49 samples of 38 cultivars with at most three lots of any cultivar; the confounding of region with cultivar genetics, breeding objective, product form and measurement campaign, which no statistical treatment of these samples can undo; the inference of the country of growth for 21 samples; and the multiplicity of models and pretreatments examined. The last has been addressed by nested validation and by permutation tests that include the selection of the best model, and the reported geographic accuracies, although some exceed their permutation distributions, are no better than those of a baseline built on three chemical descriptors; an opposing expert would not be able to use them to support a claim of origin, and they are not offered for that purpose. The UMAP and *t*-SNE maps are the most easily misread of the outputs, and they have been shown to preserve local neighborhoods less faithfully than a three-component PCA.

None of these objections undermines the relative measurements, the homolog fractions and the α/β ratios, which are independent of the calibration route and are supported by the ICE-4 composition to within a percentage point, or the chemotype structure, which is stable under every pretreatment and clustering method examined.

A11.2 Recommendations

It is recommended, first, that the absolute scale be put on a secure footing before the contents in Table A6 are issued in any report. The simplest course is the one recommended in v1.1: a gravimetrically prepared stock solution of dimethyl sulfone, about 5 mg mL^{-1} in acid-free $CDCl_3$, used as the extraction solvent, with the quantity delivered to each vial recorded by mass rather than by volume and a relaxation delay of at least 25 s pending measurement of the T_1 values. The calibrant is then non-volatile and present in every tube, and TMS serves only as the chemical-shift reference; weighing the DMS directly into each vial is an equally sound alternative. If the transfer method is retained, each bottle should be calibrated at the start and the end of every batch, the drift between the two calibrations should be recorded and used as an acceptance criterion, the bottle should be kept closed and cold between uses, and the TMS integration window should be identical in calibration and sample spectra. In either case the ICE-4 extract should be carried through each batch with its mass and bottle recorded, with acceptance limits on the recovery of the certified α- and β-acid contents as well as on the cohumulone fraction and the α/β ratio.

Second, the method should be characterized as a method before it is used for decisions. Replicate extractions of a subset of samples, at least three extractions of each of three hops of different resin content on different days, would give the repeatability and intermediate precision; a second extraction of the residue of the first would establish the completeness of extraction; an inversion-recovery measurement on one extract would give the T_1 values of the hydroxyl protons, TMS and DMS; and the pulse angle, acquisition time, number

of transients and temperature should be recorded with every spectrum. These are the elements that an ISO/IEC 17025 validation file would require.

Third, the integration should be adapted to the chemistry. The α-acid windows should follow the concentration-dependent shifts, either by setting the boundaries at the valleys of each spectrum or by fitting the three α-acid lines, and extracts of Cryo pellets and resin extracts should be prepared at about half the mass, so that their concentrations fall in the range of the pellet extracts. The β-acid totals should be reported as the sum of the major and minor tautomers, with the δ 18.5 pair reported separately until its identity is established by an exchange spectrum of purified β-acids or by spiking with a 4-deoxy-α-acid.

Fourth, if geographic authentication is the goal, the sampling must be designed for it: authenticated lots of the same cultivars grown in different regions, ten or more lots per cultivar and region over at least two harvests, with the NMR variables extended to the xanthohumol hydroxyl signal and supplemented by the measurements that are known to carry origin information, stable isotope ratios, elements and gas-chromatographic volatiles, and with class models rather than discriminant models validated on a harvest not used for training. Until such a set exists, the NMR data are best used for what they measure well: the homolog composition and α/β ratio as a check on the declared cultivar, the α- and β-acid contents as a check on the declared analysis once the scale is secured, and the ratio of oil to resin as an index of freshness.

A12. Conclusions

The spectra of 49 hop samples, integrated over one fixed set of 22 windows and normalized to the TMS signal of the extraction solvent, have been converted into absolute contents by a DMS calibration of each of the two bottles of $CDCl_3$ used. The assumption that samples 038–050 were extracted with the second bottle (8.74 mg of DMS in 800 µL) is confirmed by the agreement of their α-acid contents with the declared values (mean ratio 1.04, range 0.82–1.23), against a ratio of 0.47 under the alternative, and those samples were retained; the assignments of the 36 survey samples are likewise confirmed, sample 022 belonging to the first bottle. The two bottles differed by a factor of 2.2 in TMS content, which is most simply explained by the loss of TMS from the older, frequently opened bottle and shows that the TMS content of a bottle cannot be assumed, and the one independent test of the absolute scale, the ICE-4 extract, failed for reasons that the records do not allow to be established. The absolute contents are therefore provisional to within about ±10 %, whereas the homolog fractions and α/β ratios, which do not depend on the calibration, reproduce the ICE-4 certificate to within one percentage point and 7 % respectively.

The spectra confirm the assignments that v1.1 inferred from its integral list, resolve the minor tautomer of adlupulone at δ 18.403, confirm that the tautomer ratio is the same for the three β-acids (about 0.45 of the major form), and show that the δ 18.5 pair consists of two homolog-specific signals tied in fixed proportion to colupulone and lupulone. The ICE-4 spectrum settles the counting rule: the β-acid totals are the sums of the major and minor tautomers, and the δ 18.5 pair is not counted. The α-acid hydroxyl signals move to low field with concentration, which biases the fixed-window adhumulone–cohumulone split of concentrated extracts by several points and calls for spectrum-specific windows or line fitting.

Of the pretreatments examined, mean-centering with Pareto scaling was the most robust, keeping the noise of a blank window below 1 % of the variance while preventing domination by humulone; level scaling and the generalized logarithm let the blank generate a spurious separation of the two measurement campaigns. In every data set and by every unsupervised method the samples are organized by amount (on the absolute scale), by the α/β ratio and by the co-homolog fraction, with an oil dimension that reflects freshness and product form; the chemotypes, β-rich, high-cohumulone and α-rich, follow the genetic lineage of the cultivars, as the grouping of the New Zealand Wakatu with its Hallertau ancestors shows. Nonlinear

embeddings reproduce these groupings but preserve neighborhoods less faithfully than three principal components. The region of growth and the region of breeding were recognized only weakly, with balanced accuracies of at most 0.59 and 0.61 against a chance level of 0.33; these exceeded their permutation distributions in some tests but were no better, by more than a few hundredths, than those of a baseline given only three chemical descriptors, the α/β ratio and the two co-homolog fractions. The product form, by contrast, was recognized almost perfectly from the absolute data, and the measurement campaign far better than geography. The NMR data measure genotype and product history, not origin.

References

1. Hoek, A. C.; Hermans-Lokkerbol, A. C. J.; Verpoorte, R. An improved NMR method for the quantification of α-acids in hops and hop products. *Phytochem. Anal.* **2001**, *12* (1), 53–57. https://doi.org/10.1002/1099-1565(200101/02)12:1<53::AID-PCA550>3.0.CO;2-E

2. Killeen, D. P.; Watkins, O. C.; Sansom, C. E.; Andersen, D. H.; Gordon, K. C.; Perry, N. B. Fast sampling, analyses and chemometrics for plant breeding: bitter acids, xanthohumol and terpenes in lupulin glands of hops (*Humulus lupulus*). *Phytochem. Anal.* **2017**, *28* (1), 50–57. https://doi.org/10.1002/pca.2642

3. Bertelli, D.; Brighenti, V.; Marchetti, L.; Reik, A.; Pellati, F. Nuclear magnetic resonance and high-performance liquid chromatography techniques for the characterization of bioactive compounds from *Humulus lupulus* L. (hop). *Anal. Bioanal. Chem.* **2018**, *410* (15), 3521–3531. https://doi.org/10.1007/s00216-018-0851-y

4. Molyneux, R. J.; Wong, Y.-I. Nuclear magnetic resonance spectroscopic determination of α- and β-acid homolog composition in hops. *J. Agric. Food Chem.* **1975**, *23* (6), 1201–1204. https://doi.org/10.1021/jf60202a012

5. Yakima Chief Hops. *Commercial Cryo Hops*®; product information; Yakima, WA. https://www.yakimachief.com/commercial-cryo-hops (accessed September 23, 2026).

6. Li, J.; Li, N.; Li, X.; Chen, G.; Wang, C.; Lin, B.; Hou, Y. Characteristic α-acid derivatives from *Humulus lupulus* with antineuroinflammatory activities. *J. Nat. Prod.* **2017**, *80* (12), 3081–3092. https://doi.org/10.1021/acs.jnatprod.6b00921

7. Shannon, P. V. R.; Lloyd, R. O. V.; Cahill, D. M. Direct analysis of individual analogues of alpha-acids, beta-acids and 4-desoxyhumulones in hops using gas-liquid chromatography and nuclear magnetic resonance spectroscopy. *J. Inst. Brew.* **1969**, *75* (4), 376–382. https://doi.org/10.1002/j.2050-0416.1969.tb03230.x

8. Goese, M.; Kammhuber, K.; Bacher, A.; Zenk, M. H.; Eisenreich, W. Biosynthesis of bitter acids in hops. *Eur. J. Biochem.* **1999**, *263* (2), 447–454. https://doi.org/10.1046/j.1432-1327.1999.00518.x

9. Farag, M. A.; Porzel, A.; Schmidt, J.; Wessjohann, L. A. Metabolite profiling and fingerprinting of commercial cultivars of *Humulus lupulus* L. (hop): a comparison of MS and NMR methods in metabolomics. *Metabolomics* **2012**, *8* (3), 492–507. https://doi.org/10.1007/s11306-011-0335-y

10. Pauli, G. F.; Gödecke, T.; Jaki, B. U.; Lankin, D. C. Quantitative ^{1}H NMR. Development and potential of an analytical method: an update. *J. Nat. Prod.* **2012**, *75* (4), 834–851. https://doi.org/10.1021/np200993k

11. Malz, F.; Jancke, H. Validation of quantitative NMR. *J. Pharm. Biomed. Anal.* **2005**, *38* (5), 813–823. https://doi.org/10.1016/j.jpba.2005.01.043

12. Mo, H.; Raftery, D. Solvent Signal as an NMR Concentration Reference. *Anal. Chem.* **2008**, *80* (24), 9835–9839. https://doi.org/10.1021/ac801938j

13. Pierens, G. K.; Carroll, A. R.; Davis, R. A.; Palframan, M. E.; Quinn, R. J. Determination of analyte concentration using the residual solvent resonance in ^{1}H NMR spectroscopy. *J. Nat. Prod.* **2008**, *71* (5), 810–813. https://doi.org/10.1021/np8000046

14. Wider, G.; Dreier, L. Measuring Protein Concentrations by NMR Spectroscopy. *J. Am. Chem. Soc.* **2006**, *128* (8), 2571–2576. https://doi.org/10.1021/ja055336t

15. Akoka, S.; Barantin, L.; Trierweiler, M. Concentration Measurement by Proton NMR Using the ERETIC Method. *Anal. Chem.* **1999**, *71* (13), 2554–2557. https://doi.org/10.1021/ac981422i

16. Fulmer, G. R.; Miller, A. J. M.; Sherden, N. H.; Gottlieb, H. E.; Nudelman, A.; Stoltz, B. M.; Bercaw, J. E.; Goldberg, K. I. NMR Chemical Shifts of Trace Impurities: Common Laboratory Solvents, Organics, and Gases in Deuterated Solvents Relevant to the Organometallic Chemist. *Organometallics* **2010**, *29* (9), 2176–2179. https://doi.org/10.1021/om100106e

17. Nickerson, G. B.; Likens, S. T. Hop Storage Index. *J. Am. Soc. Brew. Chem.* **1979**, *37* (4), 184–187. https://doi.org/10.1094/asbcj-37-0184

18. Mikyška, A.; Krofta, K. Assessment of changes in hop resins and polyphenols during long-term storage. *J. Inst. Brew.* **2012**, *118* (3), 269–279. https://doi.org/10.1002/jib.40

19. American Society of Brewing Chemists. Hops-6: α-Acids and β-acids in hops and hop pellets by spectrophotometry. In *ASBC Methods of Analysis*; ASBC: St. Paul, MN (online edition).

20. American Society of Brewing Chemists. Hops-14: α-Acids and β-acids in hops and hop extracts by HPLC (International Method). In *ASBC Methods of Analysis*; ASBC: St. Paul, MN (online edition).

21. Wells, R. J.; Cheung, J.; Hook, J. M. Dimethylsulfone as a universal standard for analysis of organics by QNMR. *Accredit. Qual. Assur.* **2004**, *9* (8), 450–456. https://doi.org/10.1007/s00769-004-0779-0

22. Westwood, S.; Stoppacher, N.; Garrido, B.; Huang, T.; Saito, T.; Un, I.; Yamazaki, T.; Zhang, W. *Internal Standard Reference Data for qNMR: Dimethyl Sulfone [ISRD-02]*; Rapport BIPM-2018/04; Bureau International des Poids et Mesures: Sèvres, France, 2018.

23. Rundlöf, T.; Mathiasson, M.; Bekiroglu, S.; Hakkarainen, B.; Bowden, T.; Arvidsson, T. Survey and qualification of internal standards for quantification by ^{1}H NMR spectroscopy. *J. Pharm. Biomed. Anal.* **2010**, *52* (5), 645–651. https://doi.org/10.1016/j.jpba.2010.02.007

24. van den Berg, R. A.; Hoefsloot, H. C. J.; Westerhuis, J. A.; Smilde, A. K.; van der Werf, M. J. Centering, scaling, and transformations: improving the biological information content of metabolomics data. *BMC Genomics* **2006**, *7* (1), 142. https://doi.org/10.1186/1471-2164-7-142

25. Keun, H. C.; Ebbels, T. M. D.; Antti, H.; Bollard, M. E.; Beckonert, O.; Holmes, E.; Lindon, J. C.; Nicholson, J. K. Improved analysis of multivariate data by variable stability scaling: application to NMR-based metabolic profiling. *Anal. Chim. Acta* **2003**, *490* (1-2), 265–276. https://doi.org/10.1016/s0003-2670(03)00094-1

26. Craig, A.; Cloarec, O.; Holmes, E.; Nicholson, J. K.; Lindon, J. C. Scaling and normalization effects in NMR spectroscopic metabonomic data sets. *Anal. Chem.* **2006**, *78* (7), 2262–2267. https://doi.org/10.1021/ac0519312

27. Parsons, H. M.; Ludwig, C.; Günther, U. L.; Viant, M. R. Improved classification accuracy in 1- and 2-dimensional NMR metabolomics data using the variance stabilising generalised logarithm transformation. *BMC Bioinformatics* **2007**, *8* (1), 234. https://doi.org/10.1186/1471-2105-8-234

28. Aitchison, J. The Statistical Analysis of Compositional Data. *J. R. Stat. Soc. B* **1982**, *44* (2), 139–160. https://doi.org/10.1111/j.2517-6161.1982.tb01195.x

29. Bro, R.; Kjeldahl, K.; Smilde, A. K.; Kiers, H. A. L. Cross-validation of component models: A critical look at current methods. *Anal. Bioanal. Chem.* **2008**, *390* (5), 1241–1251. https://doi.org/10.1007/s00216-007-1790-1

30. Jackson, D. A. Stopping Rules in Principal Components Analysis: A Comparison of Heuristical and Statistical Approaches. *Ecology* **1993**, *74* (8), 2204–2214. https://doi.org/10.2307/1939574

31. Jackson, J. E.; Mudholkar, G. S. Control Procedures for Residuals Associated With Principal Component Analysis. *Technometrics* **1979**, *21* (3), 341–349. https://doi.org/10.1080/00401706.1979.10489779

32. Jolliffe, I. T.; Cadima, J. Principal component analysis: a review and recent developments. *Philos. Trans. R. Soc. A* **2016**, *374* (2065), 20150202. https://doi.org/10.1098/rsta.2015.0202

33. Ward, J. H. Hierarchical Grouping to Optimize an Objective Function. *J. Am. Stat. Assoc.* **1963**, *58* (301), 236–244. https://doi.org/10.1080/01621459.1963.10500845

34. Rousseeuw, P. J. Silhouettes: A graphical aid to the interpretation and validation of cluster analysis. *J. Comput. Appl. Math.* **1987**, *20*, 53–65. https://doi.org/10.1016/0377-0427(87)90125-7

35. Hennig, C. Cluster-wise assessment of cluster stability. *Comput. Stat. Data Anal.* **2007**, *52* (1), 258–271. https://doi.org/10.1016/j.csda.2006.11.025

36. Hubert, L.; Arabie, P. Comparing partitions. *J. Classif.* **1985**, *2* (1), 193–218. https://doi.org/10.1007/bf01908075

37. McInnes, L.; Healy, J.; Saul, N.; Großberger, L. UMAP: Uniform Manifold Approximation and Projection. *J. Open Source Softw.* **2018**, *3* (29), 861. https://doi.org/10.21105/joss.00861

38. van der Maaten, L.; Hinton, G. Visualizing data using t-SNE. *J. Mach. Learn. Res.* **2008**, *9*, 2579–2605. https://www.jmlr.org/papers/v9/vandermaaten08a.html

39. Venna, J.; Kaski, S. Neighborhood preservation in nonlinear projection methods: an experimental study. In *Artificial Neural Networks — ICANN 2001*; Lecture Notes in Computer Science; Springer: Berlin, Heidelberg, 2001; pp 485–491. https://doi.org/10.1007/3-540-44668-0_68

40. Kobak, D.; Berens, P. The art of using t-SNE for single-cell transcriptomics. *Nat. Commun.* **2019**, *10* (1), 5416. https://doi.org/10.1038/s41467-019-13056-x

41. Chari, T.; Pachter, L. The specious art of single-cell genomics. *PLoS Comput. Biol.* **2023**, *19* (8), e1011288. https://doi.org/10.1371/journal.pcbi.1011288

42. Barker, M.; Rayens, W. Partial least squares for discrimination. *J. Chemom.* **2003**, *17* (3), 166–173. https://doi.org/10.1002/cem.785

43. Brereton, R. G.; Lloyd, G. R. Partial least squares discriminant analysis: taking the magic away. *J. Chemom.* **2014**, *28* (4), 213–225. https://doi.org/10.1002/cem.2609

44. Cortes, C.; Vapnik, V. Support-vector networks. *Mach. Learn.* **1995**, *20* (3), 273–297. https://doi.org/10.1007/bf00994018

45. Ledoit, O.; Wolf, M. A well-conditioned estimator for large-dimensional covariance matrices. *J. Multivar. Anal.* **2004**, *88* (2), 365–411. https://doi.org/10.1016/s0047-259x(03)00096-4

46. Breiman, L. Random Forests. *Mach. Learn.* **2001**, *45* (1), 5–32. https://doi.org/10.1023/a:1010933404324

47. Wold, S.; Sjöström, M. SIMCA: a method for analyzing chemical data in terms of similarity and analogy. In *Chemometrics: Theory and Application*; ACS Symposium Series 52; American Chemical Society: Washington, DC, 1977; pp 243–282. https://doi.org/10.1021/bk-1977-0052.ch012

48. Varma, S.; Simon, R. Bias in error estimation when using cross-validation for model selection. *BMC Bioinformatics* **2006**, *7* (1), 91. https://doi.org/10.1186/1471-2105-7-91

49. Westerhuis, J. A.; Hoefsloot, H. C. J.; Smit, S.; Vis, D. J.; Smilde, A. K.; van Velzen, E. J. J.; van Duijnhoven, J. P. M.; van Dorsten, F. A. Assessment of PLSDA cross validation. *Metabolomics* **2008**, *4* (1), 81–89. https://doi.org/10.1007/s11306-007-0099-6

50. Szymańska, E.; Saccenti, E.; Smilde, A. K.; Westerhuis, J. A. Double-check: validation of diagnostic statistics for PLS-DA models in metabolomics studies. *Metabolomics* **2012**, *8* (S1), 3–16. https://doi.org/10.1007/s11306-011-0330-3

51. Pedregosa, F.; Varoquaux, G.; Gramfort, A.; Michel, V.; Thirion, B.; Grisel, O.; Blondel, M.; Prettenhofer, P.; Weiss, R.; Dubourg, V.; Vanderplas, J.; Passos, A.; Cournapeau, D.; Brucher, M.; Perrot, M.; Duchesnay, É. Scikit-learn: machine learning in Python. *J. Mach. Learn. Res.* **2011**, *12*, 2825–2830. https://www.jmlr.org/papers/v12/pedregosa11a.html

52. NZ Hops Ltd. *Wakatu™ variety information*; product page; Nelson, New Zealand. https://nzhops.co.nz/products/wakatu-1 (accessed September 23, 2026).

53. Ocvirk, M.; Ogrinc, N.; Košir, I. J. Determination of the geographical and botanical origin of hops (*Humulus lupulus* L.) using stable isotopes of C, N, and S. *J. Agric. Food Chem.* **2018**, *66* (8), 2021–2026. https://doi.org/10.1021/acs.jafc.7b06010

54. Pepi, S.; Chicca, M.; Telloli, C.; Di Roma, A.; Grisenti, P.; Tessari, U.; Vaccaro, C. Discrimination of geographical origin of hop (*Humulus lupulus* L.) using geochemical elements combined with statistical analysis. *Environ. Geochem. Health* **2019**, *41* (3), 1559–1576. https://doi.org/10.1007/s10653-018-0232-7

55. Silva Dias, G.; Gallon, M. E.; Gobbo-Neto, L. Comparative analysis of four hop cultivars grown in Brazil and the USA by GC-MS-based metabolomics. *J. Inst. Brew.* **2024**, *130* (4), 238–249. https://doi.org/10.58430/jib.v130i4.62

56. Green, C. P. Comparison of Tettnanger, Saaz, Hallertau and Fuggle hops grown in the USA, Australia and Europe. *J. Inst. Brew.* **1997**, *103* (4), 239–243. https://doi.org/10.1002/j.2050-0416.1997.tb00951.x

57. Van Holle, A.; Muylle, H.; Haesaert, G.; Naudts, D.; De Keukeleire, D.; Roldán-Ruiz, I.; Van Landschoot, A. Relevance of hop terroir for beer flavour. *J. Inst. Brew.* **2021**, *127* (3), 238–247. https://doi.org/10.1002/jib.648

58. Oliveri, P.; Downey, G. Multivariate class modeling for the verification of food-authenticity claims. *TrAC, Trends Anal. Chem.* **2012**, *35*, 74–86. https://doi.org/10.1016/j.trac.2012.02.005

59. Rodionova, O. Y.; Titova, A. V.; Pomerantsev, A. L. Discriminant analysis is an inappropriate method of authentication. *TrAC, Trends Anal. Chem.* **2016**, *78*, 17–22. https://doi.org/10.1016/j.trac.2016.01.010

Summary

This addendum to PNA-WP-2026-HOPS-01 reports the direct quantitative ^{1}H NMR analysis of 49 hop samples and the chemometric analysis of the resulting data. The spectra, recorded at 300 MHz on $CDCl_3$ extracts of about 100 mg of hops, were integrated over one fixed set of twenty-two windows, eighteen in the chelated enolic hydroxyl region, three in the olefinic region and one on TMS, and were normalized so that the TMS signal equals ten units. The 36 retail samples of the survey examined in version 1.1 (set S1) were joined by thirteen recent samples (set S2): five Cryo pellets of US cultivars, six New Zealand hops including three harvests of Wakatu, and two harvests of HBC 1019. The integration limits were recovered exactly from the vector drawings of the spectra, and the traces were digitized and validated against the printed integrals, so that positions, line widths and line shapes could be measured as well as integrals.

The absolute scale was established by a TMS-transferred dimethyl sulfone calibration, in which a weighed quantity of DMS was dissolved in 800 µL of each of the two bottles of $CDCl_3$ used for the extractions and the TMS signal of each sample carried the calibration of its bottle to the sample spectrum. The calibration factors were 1.2431×10^{-3} and 2.7373×10^{-3} mmol of ^{1}H per normalized unit, which correspond to TMS contents of 1.29 and 2.85 mM, a ratio of 2.20 that is most simply explained by the evaporative loss of TMS from the older, frequently opened bottle. That difference made the assignment of every sample to its bottle testable against the declared α-acid contents. For samples 038–050 the assumption of 8.74 mg of DMS gave a mean ratio of measured to declared α-acids of 1.04 (0.82–1.23), whereas the alternative would have placed every one of these recent samples below 56 % of its label; the assumption was confirmed and the samples

retained. The assignments of the S1 samples, including that of sample 022, whose entry had been duplicated, were confirmed in the same way. The S1 samples contained about three quarters of their declared α-acids and a still smaller share of their oil, as expected of older retail material, and the S1 labels therefore could not validate the absolute scale. The ICE-4 extract, the one independent check, reproduced its certified composition closely but failed in absolute terms, and because its record lacks a bottle and carries the mass of another sample, 026, the failure is attributed provisionally to the record rather than to the method. The quantified components of uncertainty combine to 2.9–3.8 %, but the stability of the transfer standard, exchange of the enolic protons and the completeness of extraction could not be quantified, and the absolute contents are best regarded as provisional to within about ±10 % until the ICE-4 measurement has been repeated.

The spectra confirmed the assignments that version 1.1 had reached from its integral list and settled the questions it had left open. The minor tautomers of adlupulone, lupulone and colupulone were observed at δ 18.403, 18.381 and 18.294 in a common ratio of about 0.45 to the major forms. The pair at δ 18.537 and 18.511 was shown to consist of two homolog-specific signals tied to colupulone and lupulone in fixed proportion, independent of the age of the material; the ICE-4 spectrum showed that the certified values are consistent only with β-acid totals that exclude them, and the β-acid contents were therefore calculated from the major and minor tautomers alone, with a residual α/β deficit of 6.5 % relative to the certificate. The α-acid hydroxyl signals move to low field with concentration and are exchange-broadened relative to those of the β-acids, and line fitting shows that the fixed boundaries of the α-acid windows consequently overstate the adhumulone fraction of concentrated extracts, by 3.7–5.0 points in the Cryo pellets, and understate the cohumulone fraction of those extracts and of the high-cohumulone cultivars by up to 5 and 7 points respectively. Contents of 0.82–25.96 % α-acids and 1.09–13.48 % β-acids were found; the Cryo pellets agreed with their declared α-acid contents (mean ratio 1.07) and exceeded the older retail pellets of the same cultivars by factors of 2.6–3.1, and the homolog fractions of the three Wakatu harvests agreed to within 1.6 points while their amounts varied with the lot, although other same-cultivar pairs differed by up to five points.

For the chemometric analysis the integrals and the eight quantified constituents were each examined on the absolute scale and in compositional form. A comparison of sixty pretreatments against criteria that do not depend on the groupings sought showed mean-centering with Pareto scaling to be the most robust choice, since it kept the blank window below 1 % of the variance without letting humulone dominate; level scaling and the generalized logarithm, by contrast, gave the blank most of the variance and allowed its small baseline offset to separate the two measurement campaigns. Principal component analysis resolved an axis of amount, which combines resin content, lupulin enrichment and freshness, followed by the α/β balance and the co-homolog fraction, with an oil dimension that reflects the freshness and form of the product. Ward clustering of the composition gave three stable chemotypes, β-rich, high-cohumulone and α-rich, corresponding to those of version 1.1, and the placement of the New Zealand Wakatu with its Hallertau ancestors showed that the chemotype follows the lineage of the cultivar rather than the country in which it was grown. UMAP and *t*-SNE reproduced these groupings but preserved the local neighborhoods of the samples less faithfully than three principal components, and they are offered, together with the principal component scores, in an interactive three-dimensional viewer.

Supervised classification, validated by leaving out one cultivar at a time with nested tuning and tested by permutation of the labels among cultivars, recognized the product form almost perfectly from the absolute data and the measurement campaign far better than geography. The region of growth and the region of breeding were recognized with balanced accuracies of 0.34–0.61. The best of these exceeded their permutation distributions, as did PLS-DA on the absolute data, but none exceeded by more than a few

hundredths the accuracy of a baseline model given only three chemical descriptors, the α/β ratio and the two co-homolog fractions, and a model given only the declared α-acid content came within about a tenth. Whatever geographic information the data contain is the information carried by regional breeding objectives and by the history of the samples, both of which are confounded with region in this set.

The ^{1}H NMR integrals of the hydroxyl region and of the two principal terpenes therefore measure the genotype of a hop through its homolog composition and α/β ratio, and the product and its history through the amounts of resin and oil; they do not carry a separable signature of geographic origin. It is recommended that the absolute scale be secured by adding a gravimetric DMS calibrant to every tube or by calibrating each bottle at the start and end of every batch, that repeatability, completeness of extraction and relaxation times be measured as part of an ISO/IEC 17025 validation, that the α-acid windows be set from each spectrum or replaced by line fitting, and that any attempt at geographic authentication be based on a purpose-designed set of authenticated lots, class models and independent markers. All data, calculations and chemometric outputs are provided in the companion workbook, and the three-dimensional score plots in the accompanying interactive file.